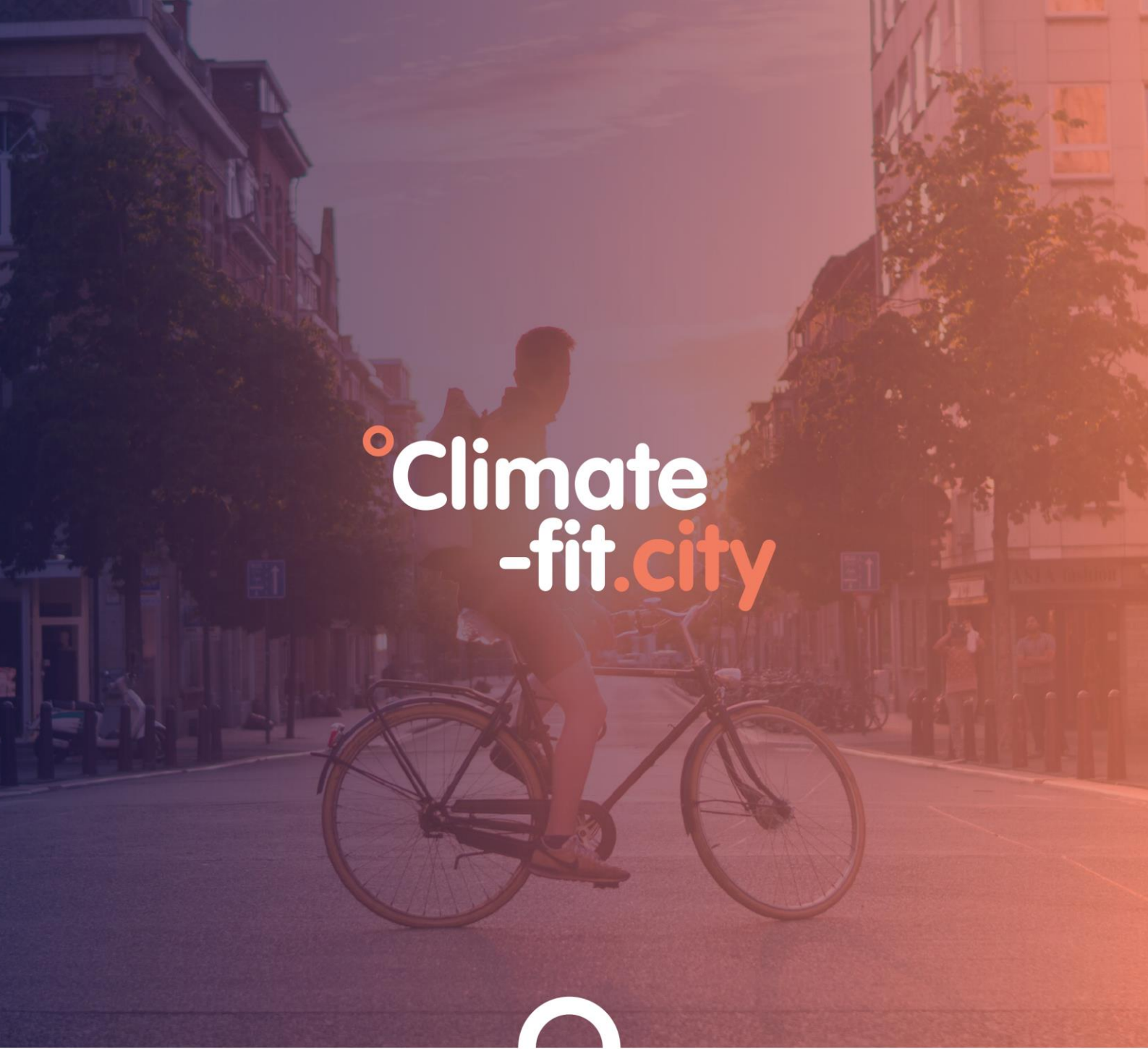

Active Mobility – Vienna

Service Report

PUCS has received funding
from the European Union's Horizon 2020
Research and Innovation Programme
under Grant Agreement No. 730004

Table of Contents

PUCS has received funding from the European Union's Horizon 2020 Research and Innovation Programme under Grant Agreement No. 730004

IMPRESSUM

Authors

Judith Köberl, JOANNEUM RESEARCH

Dominik Kortschak, JOANNEUM RESEARCH

Institutions and people involved

JOANNEUM RESEARCH LIFE	bike citizens	vito	KU LEUVEN
Judith Köberl Dominik Kortschak	Mihai Ghete Thomas Rath	Dirk Lauweat	Patrick Willems

Place and date of publication

Graz, 08/03/2019 (Version v.02)

Version history

Version	Date	Modifications
v.01	29/11/2018	-
v.02	06/03/2019	Adding of exemplary analyses from Bike Citizens Analytics; Adding of further maps on the objective climatic attractiveness; Corrections in Figure 13.b;

PUCS has received funding from the European Union's Horizon 2020 Research and Innovation Programme under Grant Agreement No. 730004

INTRODUCTION

This report is part of the *Climate-fit.city Active Mobility Service*, a prototype urban climate service. The service has been developed as part of the Climate-fit.city project (http://climate-fit.city/), which has received funding from the European Union's Horizon 2020 Research and Innovation Programme, under the Grant Agreement number 730004. The *Climate-fit.city Active Mobility Service* is supposed to support urban developers, traffic planners, public authorities, and stakeholders in their efforts to further enhance the attractiveness of active mobility in cities, particularly of urban cycling.

Active mobility, like cycling, is an important alternative to car use, especially in cities. It improves health, saves space and is environmentally friendly. The attractiveness of urban cycling is influenced by a number of factors, including, for example, safety, existing infrastructure, and convenience. Also meteorological conditions affect the behaviour of cyclists. Several studies have, for instance, found a non-linear relationship between temperature and cycling demand and a negative influence of rain and wind. Hence, climate change may alter the attractiveness of urban cycling by leading, for instance, to a rise in days with increased heat stress or to changes in (extreme) precipitation or wind patterns. Taking climatic aspects into account thus represents a relevant factor when trying to enhance the comfort and attractiveness of cycling.

This report shows how sensitively cyclists in Vienna respond to variations in meteorological conditions. Moreover, it provides information on Vienna's current and future climatic attractiveness for cycling as well as spatial and temporal variations of this attractiveness. Vienna's climatic attractiveness for cycling is assessed from both, a rather objective and a more subjective perspective. The latter is derived from the observed behaviour of cyclists in Vienna.

The report is structured into three parts. Part A presents the key data used by the *Active Mobility Service*. Part B shows the results of the analyses undertaken within the service. Part C concludes with some technical details on the methods used. Note that the analyses presented in this report have a focus on commuter traffic.

Based on the findings presented in this report, *Bike Citizens Analytics,* a tool that visualises bicycle traffic data for urban planning[1], has been enhanced by cycling-tailored climatic information. The new climatic features in *Bike Citizens Analytics* are currently implemented as a prototype version. They enable further interactive in-depth analyses to be performed on the effects of meteorological conditions on bicycle traffic.

Note that this version of the *Climate-fit.city Active Mobility Service* is a prototype that comes with a few limitations. Details on these limitations can be found in chapter 3 of this report.

[1] See e.g. https://www.bikecitizens.net/partner/cities/.

PUCS has received funding from the European Union's Horizon 2020 Research and Innovation Programme under Grant Agreement No. 730004

PART A | DATA

1 Data on bicycle traffic

Two different sources of bicycle traffic data are used in the *Active Mobility Service*: (i) data from the permanent bicycle traffic monitoring stations of the City of Vienna and (ii) data on trips tracked by the Bike Citizens App.

1.1 Bicycle traffic monitoring stations

Daily data from up to 12 permanent bicycle traffic monitoring stations – hereafter referred to as *counting stations* – are available for the period 01/01/2011 to 31/08/2017. As illustrated in Table 1, the implementation dates and, thus, the lengths of the available time series data differ according to the station. The earliest implementation date was 01/01/2011, the latest 06/09/2013. The data were provided by the City of Vienna and are also available at the platform for Open Government Data[2].

Table 1: List of permanent automatic counting stations in Vienna

Name	Date of implementation	Share in total counts (%) *)	Share in total counts on non-workdays *) / Share in total counts on workdays
Linke Wienzeile	26/01/2011	4.8	1.152
Liesingbach	17/01/2011	2.2	1.602
Operngasse	04/06/2013	16.5	0.715
Praterstern	03/06/2013	13.1	1.063
Margaritensteg	14/05/2012	4.9	1.030
Lassallestraße	01/01/2011	12.0	1.301
Neubaugürtel	06/09/2013	7.4	0.832
Langobardenstraße	01/01/2011	2.2	1.112
Opernring (inside)	20/01/2011	14.2	0.972
Opernring (outside)	14/10/2011	7.5	0.834
Donaukanal	18/01/2011	6.7	1.837
Argentinierstraße	07/02/2011	8.5	0.694

*) *for the period 01/07/2013-31/08/2017; Data source: City of Vienna – data.wien.gv.at*[3]

The fourth column in Table 1 presents the proportion between the station's share in total counts on workdays and the station's share in total counts on non-workdays. This figure helps to characterize the

[2] *Bicycle traffic census for selected routes*. Source: City of Vienna – data.wien.gv.at;
URL: https://www.data.gv.at/katalog/dataset/stadt-wien_radverkehrszhlungenderstadtwien.
[3] *Overview of all traffic count points in Vienna*; downloaded in April 2018 from
https://www.data.gv.at/katalog/dataset/stadt-wien_verkehrszhlstellenstandortewien.

PUCS has received funding from the European Union's Horizon 2020 Research and Innovation Programme under Grant Agreement No. 730004

stations with respect to leisure and commuter traffic. Values clearly above 1 suggest a comparatively high share of leisure cyclists at this station. That is, the station's share in city-wide counts on non-workdays clearly exceeds the station's share in city-wide counts on workdays. This is, for instance, the case for the station *Donaukanal*. An overview on the locations of the counting stations is given in Figure 1.

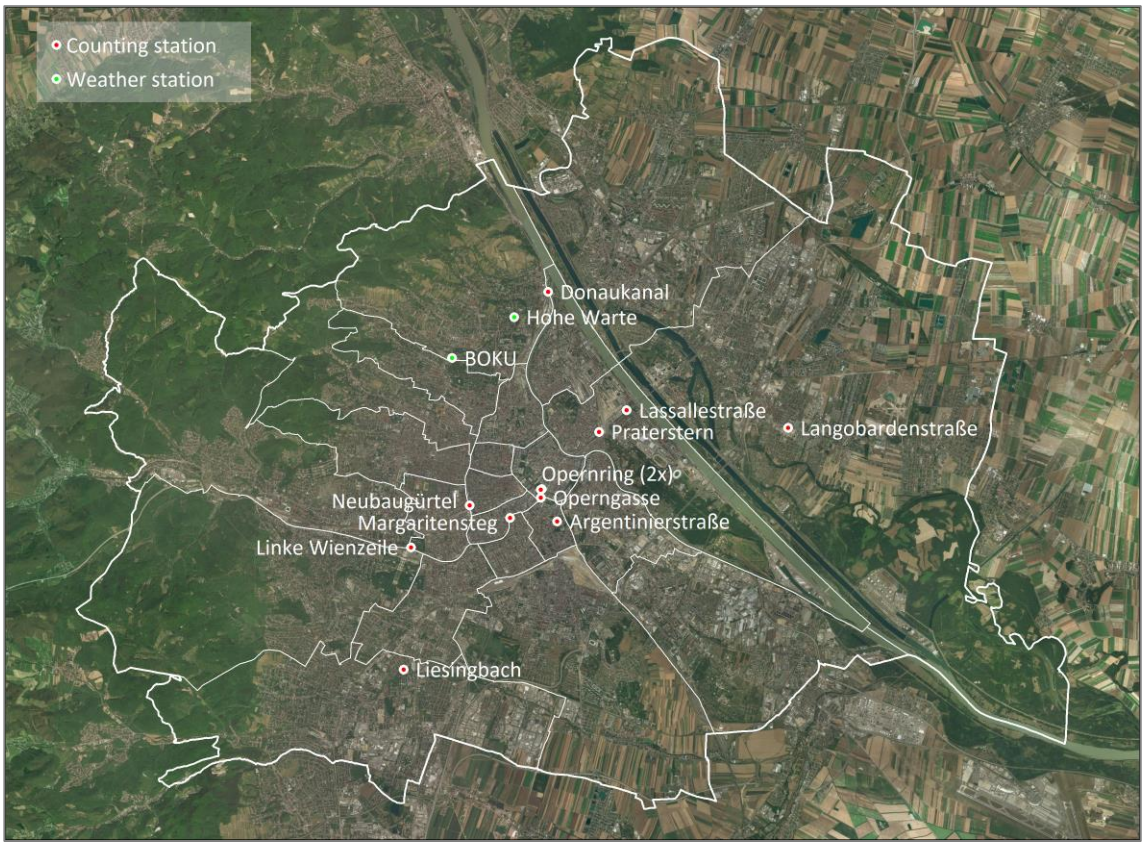

Figure 1: Location of the counting stations (and the used weather stations; see chapter 2.1). Data sources: location coordinates for counting stations from the City of Vienna – data.wien.gv.at[3]; location coordinates for weather stations from the University of Natural Resources and Life Sciences (BOKU) and the Austrian Institute for Meteorology and Geodynamics (Hohe Warte); satellite image from OpenStreetMap; administrative borders from Statistics Austria.

The plots in Figure 2 show some basic characteristics of the data measured by the counting stations. Plot (a) illustrates the average daily counts per month for the period 2011-2016. Plot (b) presents the year-to-year evolution of the average daily counts for the period 2011-2016. For reasons of consistency and comparability, only stations implemented in the year 2011 are considered. Both plots differentiate between workdays and non-workdays.

As shown in Figure 2.a, the highest average daily counts are usually observed in June, followed by July and August. The fewest cyclists typically pass the stations in January, February and December. Apart from 2013, annual average counts per day constantly increased between 2011 and 2016, at least on workdays (see Figure 2.b). On non-workdays, average counts per day additionally showed a slight decrease in 2015. Overall, workdays and non-workdays both showed an increase of 24 % between 2011 and 2016.

PUCS has received funding from the European Union's Horizon 2020 Research and Innovation Programme under Grant Agreement No. 730004

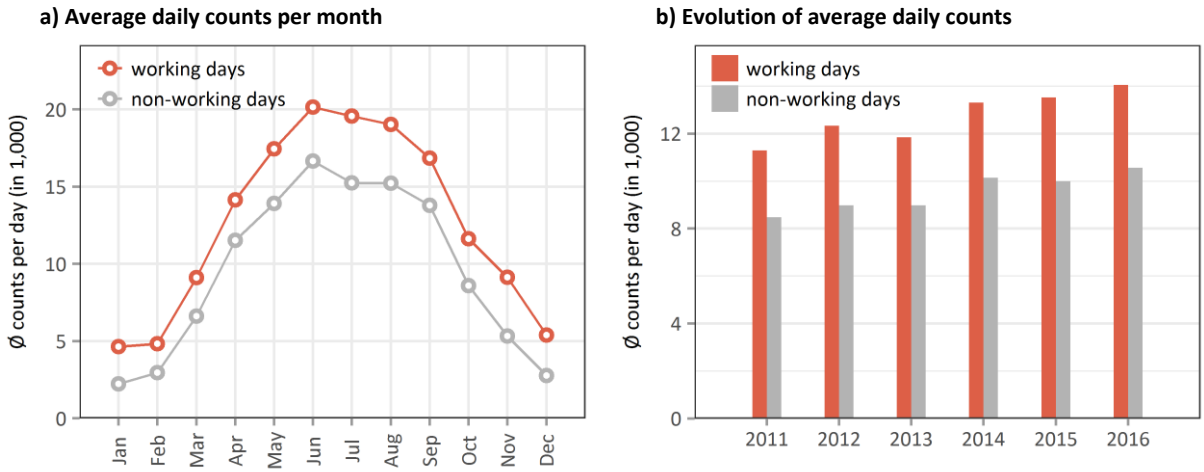

Figure 2: Some basic characteristics of the data from counting stations that were implemented in 2011. a) Average daily counts per month for the period 2011-2016. b) Evolution of average counts per day in the period 2011-2016. Data source: City of Vienna – data.wien.gv.at.[2]

In the *Active Mobility Service*, data from the counting stations are used to assess (i) how sensitively Vienna's daily bicycle traffic volume responds to variations in meteorological conditions (see chapter 4.1) and (ii) how cyclists in Vienna perceive the city's climatic attractiveness for cycling (see chapter 5.2).

1.2 Tracked trips (Bike Citizens App)

The second kind of data on bicycle traffic used by the *Active Mobility Service* is trips tracked by the Bike Citizens App. This data set includes the trips of people who used the Bike Citizens App with tracking mode in Vienna and its near surroundings between 01/01/2015 and 31/08/2017. Each track is identified by a track ID and consists of single points with the following information: longitude and latitude, metres in altitude, and time difference to the preceding point. In addition, information on the start and end time as well as the duration of each track is available. To preserve anonymity, the starting and end points are removed from the tracks.

Figure 3.a shows the evolution of the number of daily tracked trips between 01/01/2015 and 31/08/2017. For comparison, the evolution of the number of daily counts summed over all counting stations is presented in Figure 3.b. Besides the seasonal cycle, there is a considerable increase in daily tracked trips over time. This increase is mainly due to the growth in the number of users of the Bike Citizens App.

Figure 4.a illustrates the average daily tracked trips per month for the year 2016. For comparison, the monthly values of the average daily counts at all counting stations are shown in Figure 4.b. With respect to workdays, the courses of the year of tracked trips and counts at stations show many similarities: In 2016, average daily trips/counts increased from January to June, where they reached the peak of the year. After a decrease until August, they rose once again in September before falling until the end of the year. What differs, however, is the magnitude of increase or decrease in average daily trips/counts from one to the next month.

PUCS has received funding from the European Union's Horizon 2020 Research and Innovation Programme under Grant Agreement No. 730004

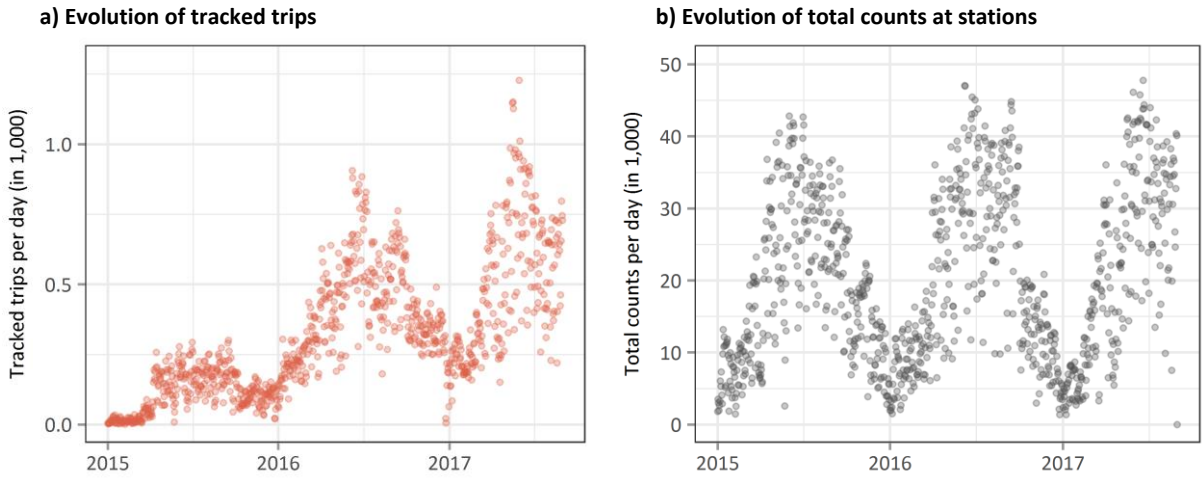

Figure 3: Evolution of the number of daily tracked trips (a) and the number of daily counts summed over all stations (b) for the period 01/01/2015-31/08/2017. Data sources: Bike Citizens and City of Vienna – data.wien.gv.at.[2]

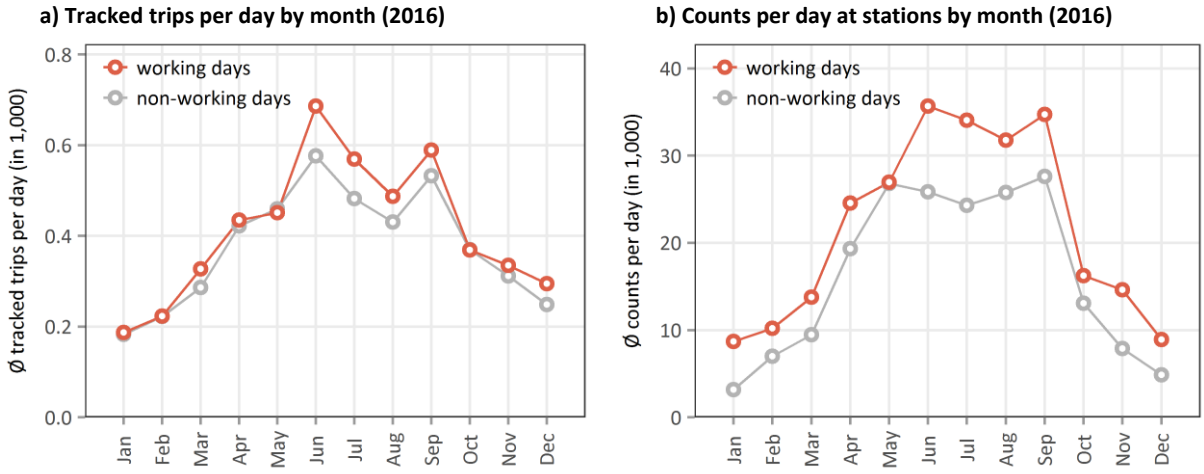

Figure 4: Tracked trips per day by month (a) and daily counts at all stations by months (b) for the year 2016. Data sources: Bike Citizens and City of Vienna – data.wien.gv.at.[2]

In the *Active Mobility Service*, tracked trips are used as an alternative source of data to quantify how sensitively Vienna's daily bicycle traffic volume responds to variations in meteorological conditions (see chapter 4.1). In addition, the data allows assessing potential spatial differences in this sensitivity (see chapter 4.3) and studying the effect of variations in meteorological conditions on average trip distance and cycling speed (see chapter 4.2). Due to the comparably small amount of tracked trips recorded in 2015, all analyses involving data on tracked trips in this prototype version of the *Active Mobility Service* are focused on the year 2016.

One of the key benefits of the data on tracked trips is their detailed spatial information. This enables analyses that would not be possible with data from counting stations. The limited period for which data is available and the limited amount of tracked trips somewhat narrow the possibilities of in-depth analyses for now. In light of the trend observed in Figure 3.a, additional in-depth analyses should, however, be possible in the near future.

PUCS has received funding from the European Union's Horizon 2020 Research and Innovation Programme under Grant Agreement No. 730004

2 Meteorological data

2.1 Meteorological data for past time horizons

The *Active Mobility Service* uses four different meteorological variables, i.e. wet-bulb globe temperature (WBGT) as a measure of thermal comfort (see Box 1), wind speed, precipitation, and snow depth. Meteorological variables related to thermal comfort, i.e. WBGT and wind speed, are simulated by the urban boundary layer climate model *UrbClim* (De Ridder et al. 2015). They are available hourly with a 100 m spatial resolution. The *UrbClim* model is driven by ERA5 (European Centre For Medium-Range Weather Forecasts 2017), the latest global reanalysis dataset produced by the European Centre for Medium-Range Weather Forecasts (ECMWF). For a brief explanation on reanalysis data see Box 2. Note that at the time of running the *UrbClim* simulations within the Climate-fit.city project only the first batch of ERA5 data, covering the period 2010-2016, had been released. When complete, the ERA5 dataset will cover the period from 1950 to present. As terrain input data *UrbClim* by default uses CORINE 2012 land use maps[4], EEA 2012 soil sealing maps[5] and MODIS satellite-based vegetation cover maps (Friedl et al. 2010). For the *Active Mobility Service*, CORINE land use maps were however replaced by the specific land use maps of the City of Vienna[6]. For further information on *UrbClim* see Lauweat et al. (2018).

Box 1: Explanation on wet-bulb globe temperature

What is the wet-bulb globe temperature?

The wet-bulb globe temperature (WBGT) is a kind of apparent temperature index and represents the ISO-standard for quantifying human thermal comfort (ISO 1989). It considers the familiar ambient (dry) temperature, the cooling ability of evaporation and wind as well as the exposure to solar radiation. The index is used by various authorities to measure thermal comfort and offer guidance with respect to workload and exercises in direct sunlight. The US National Oceanic and Atmospheric Administration (NOAA), for instance, points out that WBGT values between 29.4 °C and 31.1 °C stress the body after 30 minutes of working or exercising in direct sunlight. With WBGT values between 31.1 °C and 32.2 °C, this time span drops to 20 minutes. When WBGT values are above 32.2 °C the body is stressed after 15 minutes of physical activity[7]. For details on the calculation of WBGT within Climate-fit.city services see Lauweat et al. (2018).

Meteorological variables related to precipitation and snow depth are taken, by contrast, from local measurement stations. Precipitation data every 10 minutes come from the measurement station of the University of Natural Resources and Life Sciences (*BOKU*)[8]. Daily data on snow depth come from the weather station *Hohe Warte* of the Austrian Institute for Meteorology and Geodynamics (ZAMG)[9]. Both data are open source. The locations of the stations are illustrated in Figure 1. Table 2 summarizes the meteorological data used by the *Active Mobility Service* for Vienna.

[4] http://land.copernicus.eu/pan-european/corine-land-cover/clc-2012
[5] https://land.copernicus.eu/pan-european/high-resolution-layers/imperviousness/status-maps/2012
[6] Multipurpose map (Flächen-Mehrzweckkarte); City of Vienna – data.wien.gv.at
[7] https://www.weather.gov/tsa/wbgt
[8] Data from station *BOKU*: https://meteo.boku.ac.at/wetter/mon-archiv/,
[9] Data from station *Hohe Warte*: https://www.zamg.ac.at/cms/de/klima/klimauebersichten/jahrbuch

PUCS has received funding from the European Union's Horizon 2020 Research and Innovation Programme under Grant Agreement No. 730004

Table 2: Overview on the meteorological data used by the Active Mobility Service for Vienna

MET variable	Data source	Spatial resolution	Temporal resolution	Available period
WBGT	UrbClim-ERA5	Grid (100 m)	Hourly	2010-2016
Wind speed	UrbClim-ERA5	Grid (100 m)	Hourly	2010-2016
Precipitation	Local measurement station: *BOKU*	Point	10 minutes	2005-2017
Snow depth	Local measurement stations: *Hohe Warte*	Point	Daily	1993-2017

Box 2: Explanation on reanalysis data

What are reanalysis data?

Reanalysis data are synthesized weather records. "[They] *are produced by a numerical weather prediction (NWP) model – the same type of model used in weather forecasting – driven by historical weather observations from satellites, aircraft, balloons, and surface stations. The model and data-assimilation system are 'frozen' in time to provide as consistent a record as possible; only the observational data change. With this approach it is possible to generate a time series of gridded atmospheric variables, including temperature, pressure, wind, humidity, precipitation, and others, extending back several decades"* (Brower et al. 2013).

2.2 Meteorological data for future time horizons

The *Active Mobility Service* not only provides information on Vienna's current climatic attractiveness for cycling, but also on its projected future climatic attractiveness. This future attractiveness is assessed based on the projected climate change between the reference period 1981-2010 and the future period 2036-2065. Two different Representative Concentration Pathways (RCPs) are considered: RCP4.5 and RCP8.5 (see also Box 3).

Box 3: Explanation on Representative Concentration Pathways

What are Representative Concentration Pathways (RCPs)?

Various factors have to be taken into account when projecting the climate of the future, including the evolution of greenhouse gas emissions, technological developments, population growth, economic development, changes in land use, etc. In order to ensure the comparability of outputs from different modelling systems a standardized set of scenarios is used. RCPs are such a standardized set of scenarios. They define scenarios on possible future emissions and concentrations of greenhouse gases in the atmosphere. Overall, there are four representative pathways: RCP2.6, RCP4.5, RCP6 and RCP8.5. The number behind the RCP relates to the amount of radiative forcing produced by greenhouse gases in 2100 (Wayne 2013).

RCP4.5 is a moderate emission scenario with effective climate change mitigation measures. RCP8.5 represents the business-as-usual scenario with unbridled emissions. The future projections used in the *Active Mobility Service* consider all publicly available global and regional climate model outputs from the

PUCS has received funding from the European Union's Horizon 2020 Research and Innovation Programme under Grant Agreement No. 730004

CMIP5 and EURO-CORDEX databases[10]. The figures outlined in this service report represent the mean over these considered models, i.e. the multi-model ensemble mean. For details on the methodology of downscaling climate projections and generating the future climate data used in the *Active Mobility Service* see Lauweat et al. (2018).

3 Limitations of the prototype version

The prototype version of the *Active Mobility Service* has a few limitations that need to be considered when interpreting the tables and figures in this service report. As mentioned in chapter 2.1, ERA5 reanalyses data was only available for the period 2010-2016 when running the *UrbClim* simulations for this prototype version of the *Active Mobility Service*. All analyses based on past meteorological data are thus limited to this period. That is the reason why, in this prototype version, the statistical evaluations of the *current climate* in chapter 5 are not based on a 30-year period as common in climate statistics, but only a 7-year period. However, the climate change signals themselves were calculated based on the comparison of two 30-year periods (see chapter 2.2 and Lauweat et al. 2018). Furthermore, no climate change projections are available for the meteorological parameter *snow depth*.

[10] CMIP5 – Coupled Model Intercomparison Project Phase 5; https://cmip.llnl.gov/cmip5/
EURO-CORDEX – Coordinated Downscaling Experiment (European Domain); https://www.euro-cordex.net/

PUCS has received funding from the European Union's Horizon 2020 Research and Innovation Programme under Grant Agreement No. 730004

PART B | CYCLING – WEATHER – CLIMATE

4 Sensitivity of the city's cyclists towards meteorological conditions

This section deals with the sensitivity of Vienna's cyclists to meteorological conditions. First, we look at the cyclists' sensitivity at an aggregate – more or less city-wide – level. The effects of meteorological conditions on total bicycle traffic volume (chapter 4.1) as well as average cycling speed and trip distance (chapter 4.2) are presented. Subsequently, potential spatial differences in the sensitivity of the bicycle traffic volume towards meteorological conditions are illustrated (chapter 4.3).

4.1 Effect of meteorological conditions on total bicycle traffic volume

The *Active Mobility Service* uses a statistical model to estimate how sensitively the city's daily bicycle traffic volume (BTV) responds to variations in different meteorological indicators (see chapter 6.1 for technical details). By considering only workdays, the model primarily focuses on commuter traffic. Saturdays, Sundays and official holidays are excluded from the analysis. Two different data sources on bicycle traffic volume are used for analysing the sensitivity towards variations in meteorological conditions: data from counting stations (see chapter 1.1) and data on trips tracked by the Bike Citizens App (see chapter 1.2). This means, the city's daily bicycle traffic volume is either measured as the daily sum of counts over all considered counting stations or as the daily sum of the number of tracked trips.

In order to use the longest possible observation period whilst still remaining consistent, all counting stations that came into operation after 2011 (i.e. *Praterstern*, *Margaritensteg*, and *Neubaugürtel*) are excluded from the analyses. Counting stations characterised by a comparatively high share of recreational cyclists (i.e. *Donaukanal* and *Liesingbach*; see Table 1) are omitted as well, due to the focus on commuter traffic.

The statistical model uses a number of relevant factors to explain variations in the city's daily bicycle traffic volume (see Table 3). These include (i) socio-economic variables like the number of inhabitants, (ii) calendric variables such as school holidays, bridging days[11], weekdays and hours of daylight, and (iii) meteorological variables. Overall, the effect of four meteorological indicators is studied: mean WBGT between 06:00 and 20:00 ($WBGT_{mean}$), the maximum of mean hourly wind speeds between 06:00 and 20:00 (WS_{max}), the number of hours with precipitation between 06:00 and 20:00 (PRH), and snow depth at 07:00. As mentioned in chapter 2.1, data on precipitation and snow depth stem from local measurement stations, whereas data on WBGT and wind speed come from the urban climate model *UrbClim*. *UrbClim* output is available at a 100 m resolution. To estimate the effect of variations in meteorological conditions on total bicycle traffic volume, *cycling-weighted* city-wide averages of the respective indicators are used. The weighting is done according to the spatial distribution of bicycle traffic

[11] Bridging days are workdays that fall between a public holiday and a typical non-workday. For example a Friday that is preceded by a public holiday is a bridging day. Lots of people use them to take the day off and have a "long" weekend.

PUCS has received funding from the European Union's Horizon 2020 Research and Innovation Programme under Grant Agreement No. 730004

volume measured in terms of tracked trips. That is, those grid cells frequented more heavily by cyclists get more weight when calculating the city-wide average of the respective indicator. Table 3 summarizes the variables used in the statistical model to explain variations in the city's daily bicycle traffic volume.

Table 3: Variables used to explain variations in the city's daily bicycle traffic volume

Type	Name	Description
Socio-economic	Population	Number of the city's inhabitants per year
Calendric	Christmas holidays	A variable indicating school holidays at Christmas
Calendric	Easter holidays	A variable indicating school holidays at Easter
Calendric	Summer holidays	A variable indicating school holidays in summer
Calendric	Semester breaks	A variable indicating school holidays in February
Calendric	Bridging days	A variable indicating bridging days
Calendric	Weekday	A variable indicating the weekday (Monday, Tuesday, etc.)
Calendric	Day length	Hours of daylight
Meteorological	WBGT ($WBGT_{mean}$)	Mean wet-bulb globe temperature in °C between 06:00 and 20:00
Meteorological	Wind speed (WS_{max})	Maximum mean hourly wind speeds in km/h between 06:00 and 20:00
Meteorological	Precipitation hours (PRH)	Number of hours with precipitation > 0.1 mm between 06:00 and 20:00
Meteorological	Snow depth (SD)	Depth of snow in cm at 07:00

The applied statistical model provides the sensitivity of the city's daily BTV towards the four considered meteorological indicators. For illustrating these sensitivities, we make use of response function plots. Box 4 contains a guideline on how to read and interpret these plots.

Figure 6 shows the resulting response functions when measuring the city's daily BTV in terms of counts at stations on workdays. As illustrated in plot (a), higher WBGT values result in higher values of the city's BTV – at least up to a certain point. When rising beyond this threshold, further increases in WBGT cause the city's BTV to decrease again. According to the response function in Figure 6.a, a mean WBGT of about 25 °C during the daytime is perceived as optimal by cyclists in Vienna. In contrast, a mean WBGT of 0 °C during the daytime typically causes the city's BTV to drop by almost 70 % compared to WBGT conditions perceived as optimal (all other factors being equal). A mean WBGT of 30°C usually leads to a reduction in the city's BTV by about 9 °%. To sum up, variations in WBGT throughout the year show a considerable effect on the city's daily BTV.

The other three meteorological indicators – wind speed, precipitation and snow on the ground – all show a negative effect on the city's daily BTV, as one might expect. Variations in wind speeds exhibit the smallest impact potential (see Figure 6.b). One reason might be that the impact of the wind's cooling effect is already largely captured by WBGT (see also Box 1). Hence, what remains is the effect of an increase in air resistance in the case of a head wind. Wind variability below mean hourly speeds of about 20 km/h during the daytime has virtually no effect on the city's daily BTV. In other words, there is quite a large spectrum of wind speeds that have hardly influence on the behaviour of cyclists in Vienna. Even the effect of high wind speeds is comparably small: typically, the impact potential of wind speed remains below a 20 % reduction of the city's daily BTV. By contrast, BTV drops by about 15 % in case of one hour with precipitation during the day and by more than 60 % in case of an entirely rainy day, compared to a day with virtually no precipitation (all other factors being equal). Snow on the ground as well shows a noticeable effect on the city's BTV. Compared to a winter day with no snow, BTV drops by about 20 % in case of 1 cm and by more than 50 % in case of 10 cm snow on the ground (all other factors being equal).

PUCS has received funding from the European Union's Horizon 2020 Research and Innovation Programme under Grant Agreement No. 730004

Box 4: Interpretation guideline for response function plots

How to read a response function plot?

Throughout this chapter we use similar-looking plots to illustrate how sensitively the city's daily bicycle traffic volume (BTV) responds to variations in particular meteorological (MET) indicators. The illustrated response functions are derived from a statistical model that uses a number of relevant factors – day of the week, hours of daylight, the city's population, school holidays, WBGT, precipitation, wind, etc. – to explain variations in the city's daily BTV. The consideration of all these factors within our statistical model allows us to "control" for them and hold them fixed when plotting the response of the city's daily bicycle traffic volume to variations in a particular MET indicator. Hence, when interpreting the illustration of a response function within this chapter, be aware that it shows the response of the city's daily BTV to variations in the considered MET indicator, while holding all other factors of the model fixed.

The black line in Figure 5 represents the response of the city's daily BTV (plotted on the vertical axis) to variations in the considered MET indicator (plotted on the horizontal axis). The steeper the slope of the line, the more sensitive is the city's daily BTV to variations in the considered MET indicator. Grey-shaded areas around the black line display the confidence interval and thus reflect the uncertainty attached to the estimation of the response.

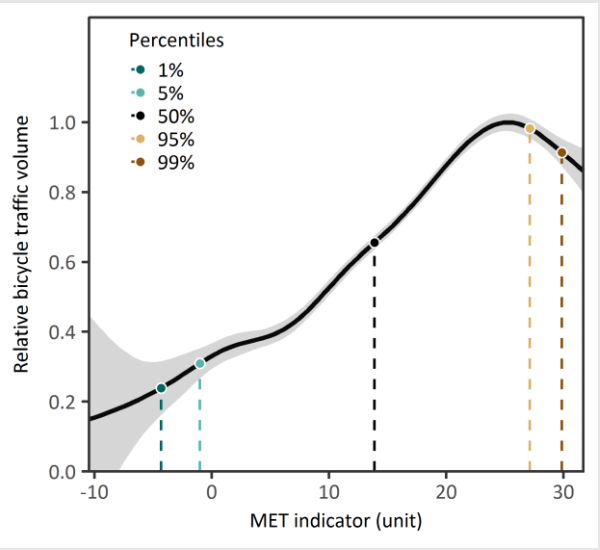

Figure 5: Example of a response function plot (design based on Marí-Dell'Olmo et al., 2018)

Note that the city's daily BTV – displayed on the vertical axis – is measured in relative terms. A value of 1 is assigned to the highest daily BTV that results from systematically varying the considered MET indicator while holding all other factors fixed. Hence, those values of the considered MET indicator that are associated with a relative BTV of 1 are perceived as *optimal* conditions for cycling by the city's cyclists. A relative BTV of, for example, 0.6 indicates a reduction by 40 % compared to the city's daily BTV under optimal conditions of the considered MET indicator.

To get an impression on how often particular values of the considered MET indicator occurred within the model calibration period, selected percentiles of the MET indicator's distribution (1 %, 5 %, 50 %, 95 %, and 99 %) are displayed in addition to the response function. The 5th percentile, for example, indicates the value of the considered MET indicator below which 5 % of all values observed within the model calibration period were found. In our example plot, 5 % of the observed values of the considered MET indicator fall below -1.2. Hence, in 5 % of days the MET indicator did not exceed -1.2, whereas in 95 % of days it exceeded this value in the calibration period. The other quantiles are to be interpreted in the same way.

PUCS has received funding from the European Union's Horizon 2020 Research and Innovation Programme under Grant Agreement No. 730004

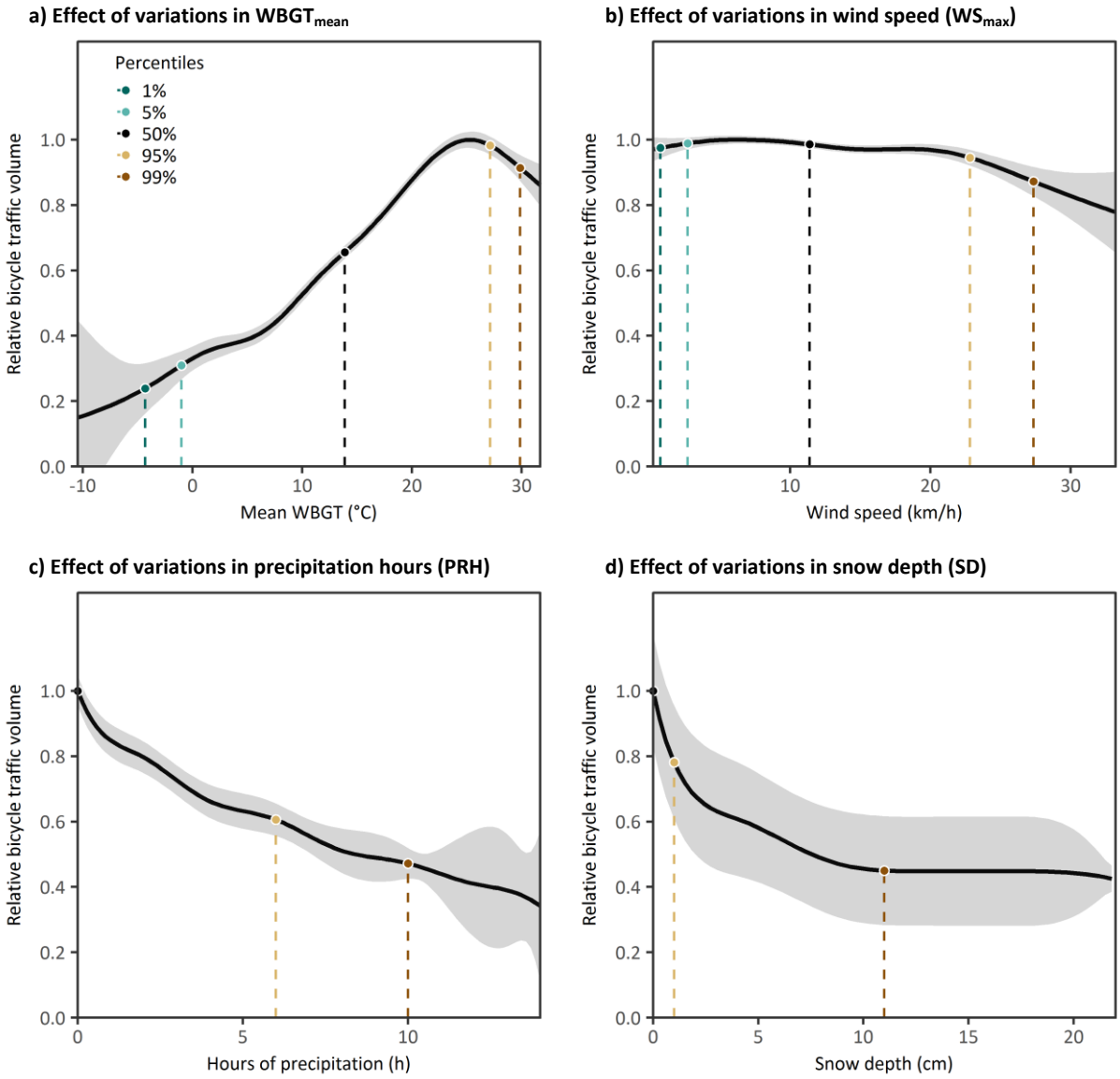

Figure 6: Effect of variations in MET indicators on the city's daily BTV, where BTV is measured in terms of counts at considered counting stations. The plots refer to workdays only. Period of model calibration: 2011-2016. Plot design based on Marí-Dell'Olmo et al. (2018).

Table 4 provides a numerical illustration of the response functions shown in Figure 6. The displayed figures refer to the effects on the city's daily BTV due to deviations of the considered meteorological indicators from the values perceived as optimal by cyclists in Vienna. As already evident from the graphical illustrations, variations in wind speeds show to have to lowest impacts on cyclists in Vienna.

PUCS has received funding from the European Union's Horizon 2020 Research and Innovation Programme under Grant Agreement No. 730004

Table 4: Effect of variations in MET indicators on the city's daily BTV, where BTV is measured in terms of counts at considered counting stations. Figures refer to working days only. Period of model calibration: 2011-2016.

$WBGT_{mean}$ [°C]	Effect on BTV [compared to optimal WBGT conditions]
30	-9 %
25	**±0 %**
20	-12 %
15	-30 %
10	-47 %
5	-61 %
0	-67 %
-5	-77 %
-10	-85 %

WS_{max} [km/h]	Effect on BTV [compared to optimal WS conditions]
0	**±0 %**
10	-1 %
15	-3 %
20	-3 %
25	-9 %
30	-17 %

PRH [h]	Effect on BTV [compared to optimal PRH conditions]
0	**±0 %**
1	-15 %
5	-37 %
10	-53 %
14	-66 %

SD [cm]	Effect on BTV [compared to optimal SD conditions]
0	**±0 %**
1	-22 %
5	-42 %
10	-54 %
20	-56 %

Additional in-depth analyses of the BTV's meteorological sensitivity reveal that the effect of precipitation varies over the course of a day. Figure 7 shows how precipitation sums of more than 1 mm within three hours affect the city's daily BTV, depending on whether taking place in the morning (06:00-09:00), at noon (11:00-14:00) or in the afternoon (16:00-19:00). Precipitation during the morning hours causes daily bicycle traffic to drop by more than 30 % compared to days with no significant precipitation amounts in the morning, at noon or in the afternoon. Precipitation at noon or in the afternoon, by contrast, only leads to a reduction of daily bicycle traffic by about 24 % or 22 %. Hence, rain in the morning clearly exceeds the effect of rain at noon or in the afternoon.

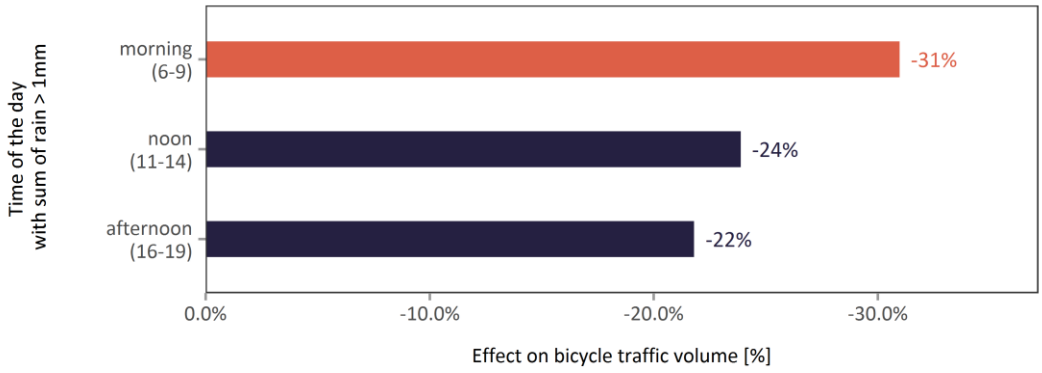

Figure 7: Effect of precipitation on the city's daily BTV, depending on the time of the day. BTV is measured in terms of counts at considered counting stations. Figures refer to workdays only. Period of model calibration: 2011-2016.

Figure 8 shows the effect of variations in meteorological indicators on the city's daily BTV when measuring BTV in terms of the number of tracked trips[12] instead of counts at stations. Note that in the prototype version of the *Active Mobility Service* only the year 2016 is available for model calibration when using tracked trips (see chapters 1.2 and 2.1). Therefore, a somewhat limited spectrum of different

[12] The statistical model using tracked trips as a measure of daily BTV additionally accounts for the increase in users of the Bike Citizens App over time (see Figure 3).

PUCS has received funding from the European Union's Horizon 2020 Research and Innovation Programme under Grant Agreement No. 730004

meteorological conditions – and hence also a limited spectrum of observed responses – is available for model calibration. This makes the estimates less robust and more prone to uncertainty and may be partially the reason for the broader confidence intervals around the response functions.

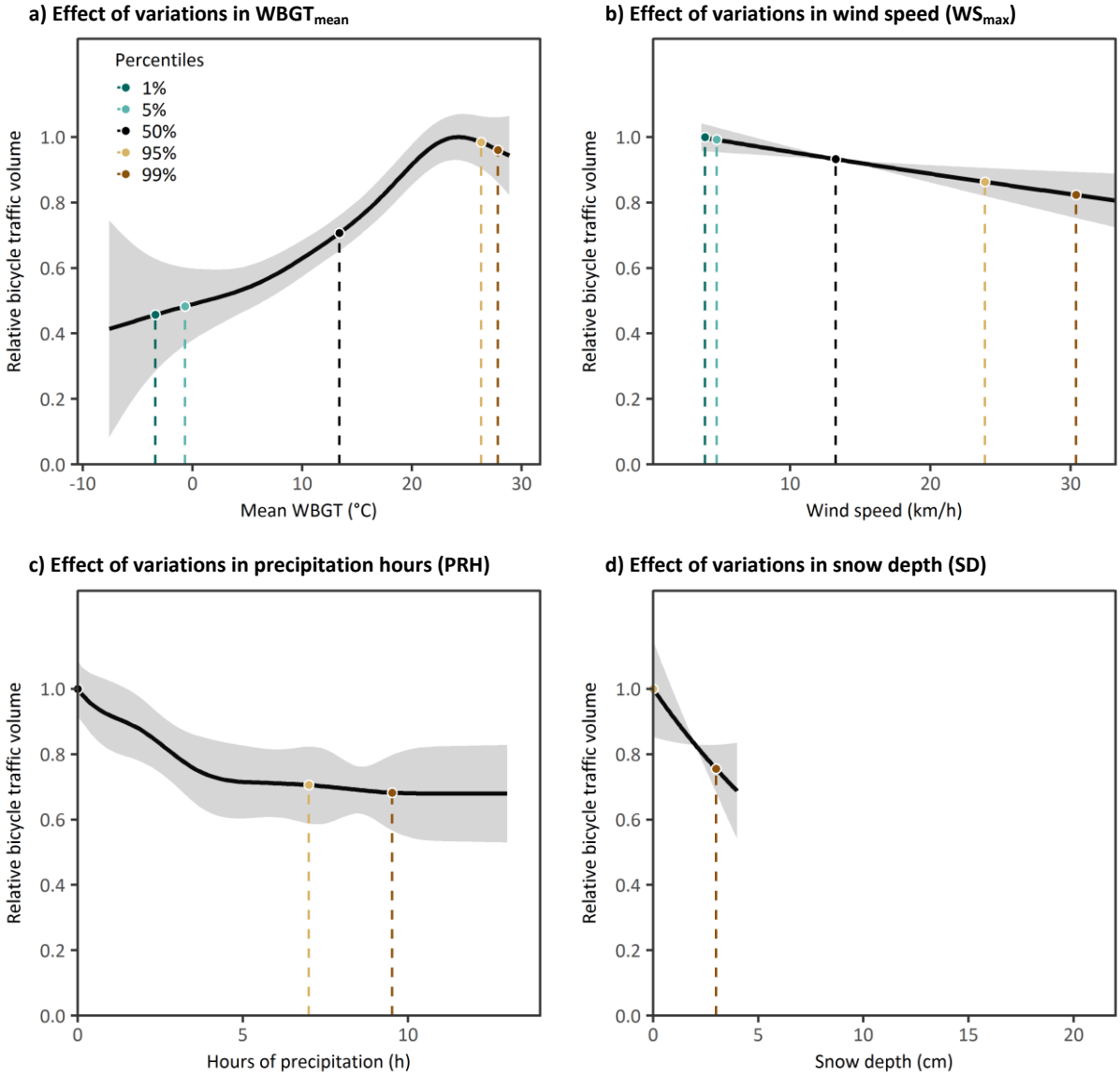

Figure 8: Effect of variations in MET indicators on the city's daily BTV, where BTV is measured in terms of the number of tracked trips. Plots refer to workdays only. Period of model calibration: 2016. Plot design based on Marí-Dell'Olmo et al. (2018).

The spectrum of daily mean WBGT, for instance, ranged from -10.6 °C to 31.2 °C between 2011 and 2016, but only from -7.7 °C to 28.6 °C in 2016. Moreover, 2016 was a year with not much snow. In the period 2011 to 2016, the maximum snow depth reached 30 cm and there were on average 13 days with snow on the ground per year. In 2016, by contrast, a maximum snow depth of only 4 cm and 9 days with snow on the ground were reported. Consequently, there were only few occasions to observe how cyclists respond to snow on the ground. That is why the information content of the estimated response function on snow depth in Figure 8.d is rather limited. Less data available for model fitting is also the reason why the

PUCS has received funding from the European Union's Horizon 2020 Research and Innovation Programme under Grant Agreement No. 730004

response to wind speed is approximated by a linear function this time (Figure 8.c). In order to prevent overfitting, the statistical model decides on a simple linear relationship instead of a more complex function to approximate the wind effect.

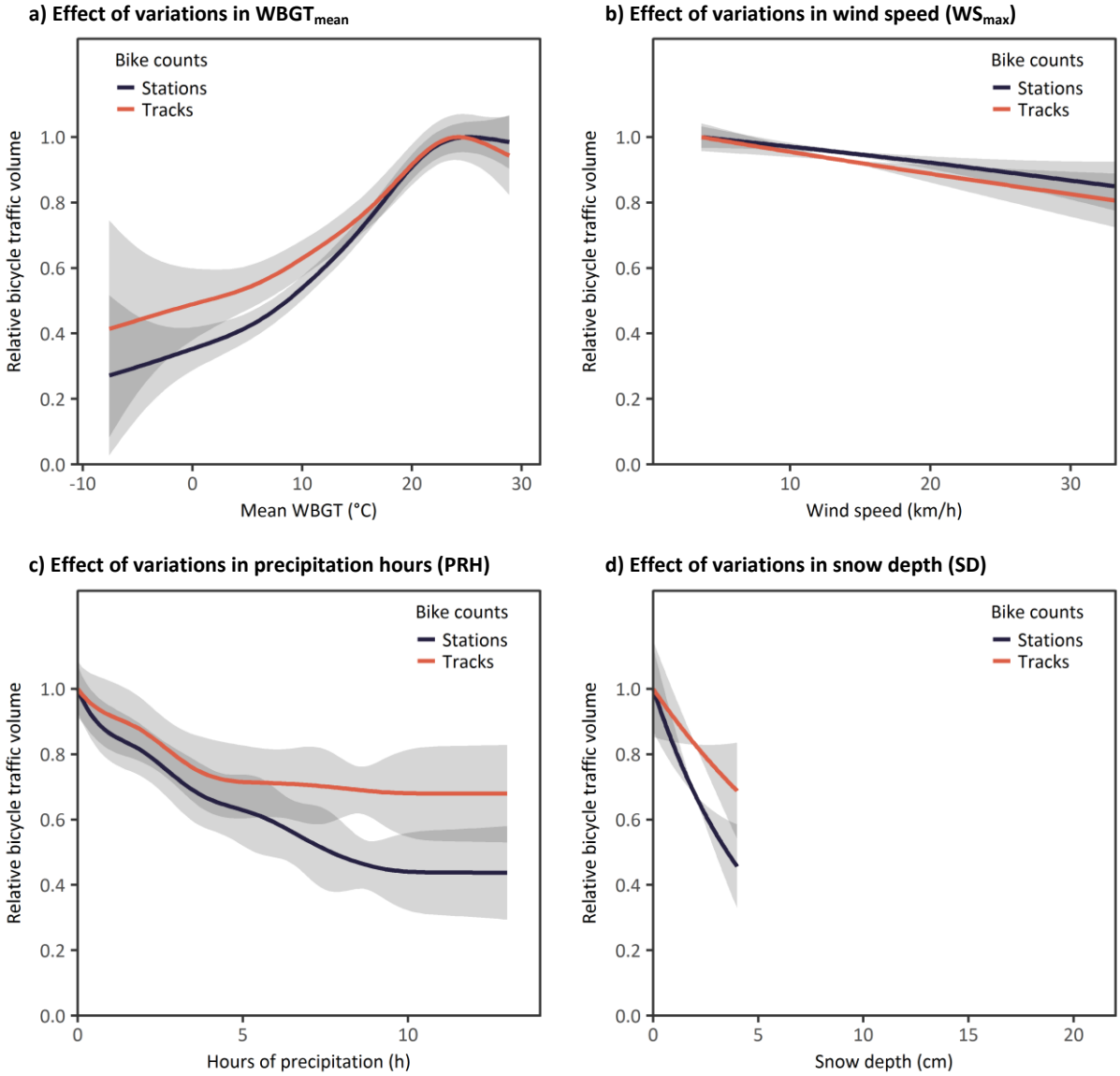

Figure 9: Effect of variations in MET indicators on the city's daily BTV, using different sources for BTV measurement: Data from measurement stations ("Stations") vs. tracked trips from Bike Citizens ("Tracks"). Plots refer to workdays only. Period of model calibration: 2016.

The group characteristics of cyclists tracking their trips may differ from the group characteristics of cyclists captured by the counting stations (e.g. smaller fraction of elderly people, etc.). The same holds true for the sensitivity towards meteorological conditions. To allow for comparisons between the sensitivity of tracked trips and the sensitivity of counts at stations, Figure 9 shows the respective response functions for the model calibration period 2016. As long as the grey-shaded areas around the response functions overlap, differences between the two curves are not statistically significant. With few exceptions, cyclists tracking their trips show a somewhat lower sensitivity towards variations in

PUCS has received funding from the European Union's Horizon 2020 Research and Innovation Programme under Grant Agreement No. 730004

meteorological conditions than cyclists captured by the counting stations. However, most of the differences are statistically not significant. Note again, that especially the results for snow depth are to be interpreted with caution due to the little amount of observational experience available for 2016.

Figure 10 once again illustrates the response functions of the city's daily BTV, with BTV being measured in terms of counts at stations. The dark-blue lines indicate the response functions that result from using all available years, i.e. 2011-2016, for model calibration. The orange-red lines, by contrast, display the response functions that result from using only the year 2016 for model calibration.

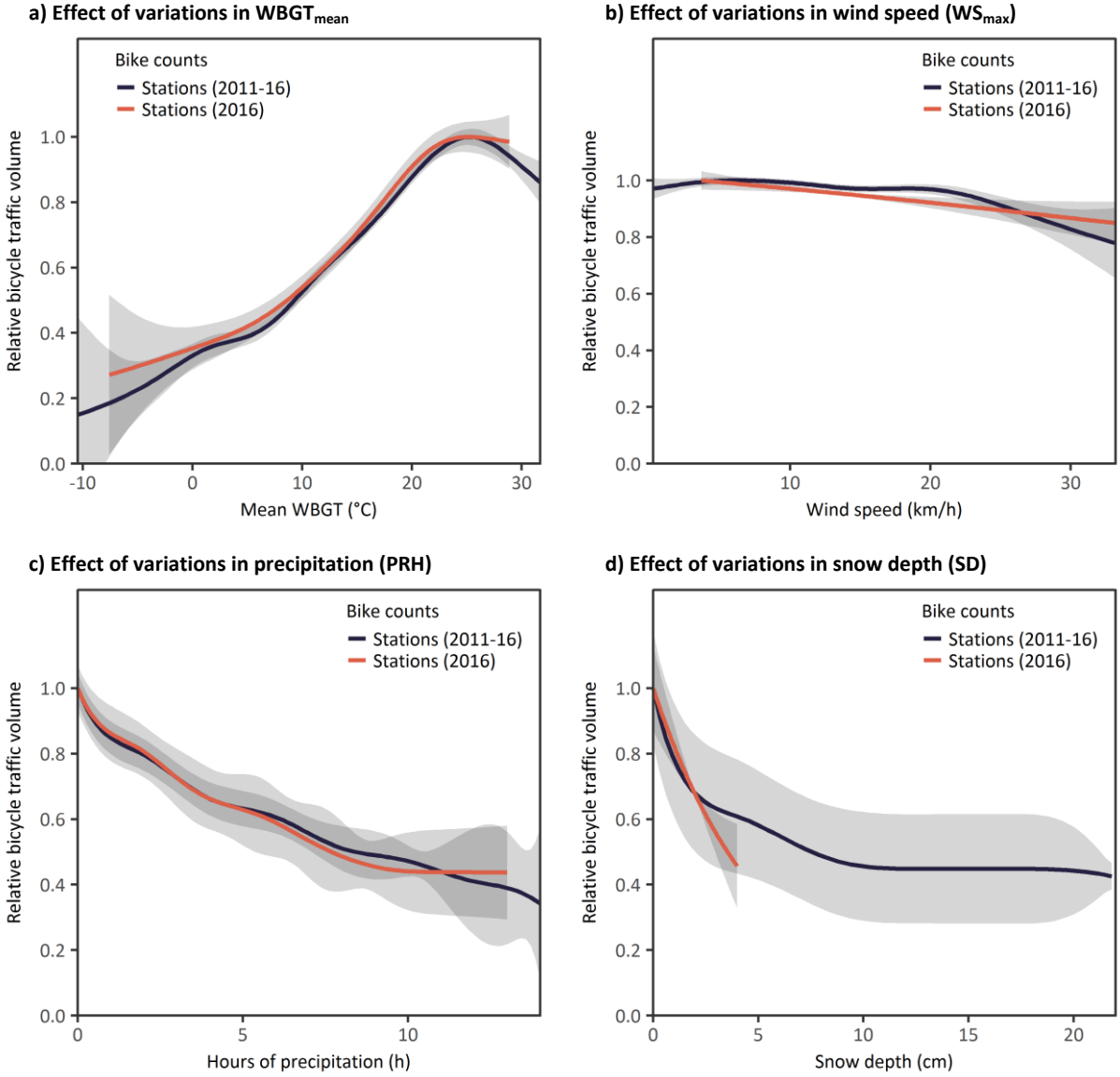

Figure 10: Effect of variations in MET indicators on the city's daily BTV, where BTV is measured in terms of counts at considered counting stations. Comparison of two different periods of model calibration: 2011-2016 and 2016. Plots refer to workdays only.

Table 5 illustrates the role and importance of the meteorological indicators in explaining variations in the city's daily BTV. The adjusted R^2 has values between 0 and 1 and indicates how much of the observed variation in the city's daily BTV can be explained by the applied statistical model. When measuring BTV in

PUCS has received funding from the European Union's Horizon 2020 Research and Innovation Programme under Grant Agreement No. 730004

terms of counts at stations and using the period 2011 to 2016 for calibrating the model, almost 95 % of the variation in the city's daily BTV can be explained. Without considering any meteorological indicators, the model would only be able to explain 65 % of the BTV's variation. By additionally taking meteorological conditions into account, the model is able to explain 84 % of the variance that would remain unexplained otherwise.

Table 5: 'Explained variation' (adj. R^2) and improvement in 'explained variation' due to the consideration of MET indicators

BVT measured by …	Period of model calibration	Adj. R^2 (model with MET)	Adj. R^2 (model without MET)	Change in adj. R^2 due to MET
… counting stations	2011-2016	0.944	0.650	+0.293
… counting stations	2016	0.947	0.649	+0.299
… tracked trips	2016	0.841	0.605	+0.236

In the case of tracked trips, the improvement due to additionally considering meteorological conditions is somewhat less pronounced. The amount of explained variation in BTV rises from 61 % to 84 %. This means, that 60 % of the otherwise still unexplained variance can be explained by additionally taking meteorological conditions into account.

4.2 Effect of meteorological conditions on trip distance and cycling speed

The data on tracked trips also allow investigating the effect of variations in meteorological conditions on average trip distance and average cycling speed. Again, statistical models are used to estimate how sensitive average trip distance and average cycling speed are to variations in meteorological conditions. The models work on a daily resolution and only consider workdays.

Figure 11 illustrates the response functions for those meteorological indicators that show a statistically significant influence on either average trip distance or average cycling speed. The vertical axis on the left side of each plot measures average trip distance or cycling speed in relative terms. The value 1 represents the highest average trip distance or cycling speed that results from systematically varying the considered meteorological indicator while holding all other factors fixed. The vertical axes on the right side, by contrast, measures average trip distance or cycling speed in absolute terms.

There is a notable influence of WBGT and precipitation on average trip distance. As shown in Figure 11.a, average trip distance increases with WBGT. With mean WBGT below 0°C during daytime average trip distance drops by about 50 % compared to days with WBGT values perceived as optimal by the cyclists (all other factors being equal). Expressed in absolute terms, average trip distance drops below 2.8 km with mean WBGT being less than 0 °C during daytime (and no hours of precipitation). For comparison, average trip distance amounts to 5.4 km on days with meteorological conditions perceived as optimal.

In contrast to WBGT, the duration of precipitation shows a negative effect on average trip distance (see Figure 11.b). Five hours with precipitation cause a reduction in the average trip distance by about 15 % compared to days with virtually no precipitation (all other factors being equal). Days with ten hours of precipitation cause the average trip distance to be reduced by about 28 %.

PUCS has received funding from the European Union's Horizon 2020 Research and Innovation Programme under Grant Agreement No. 730004

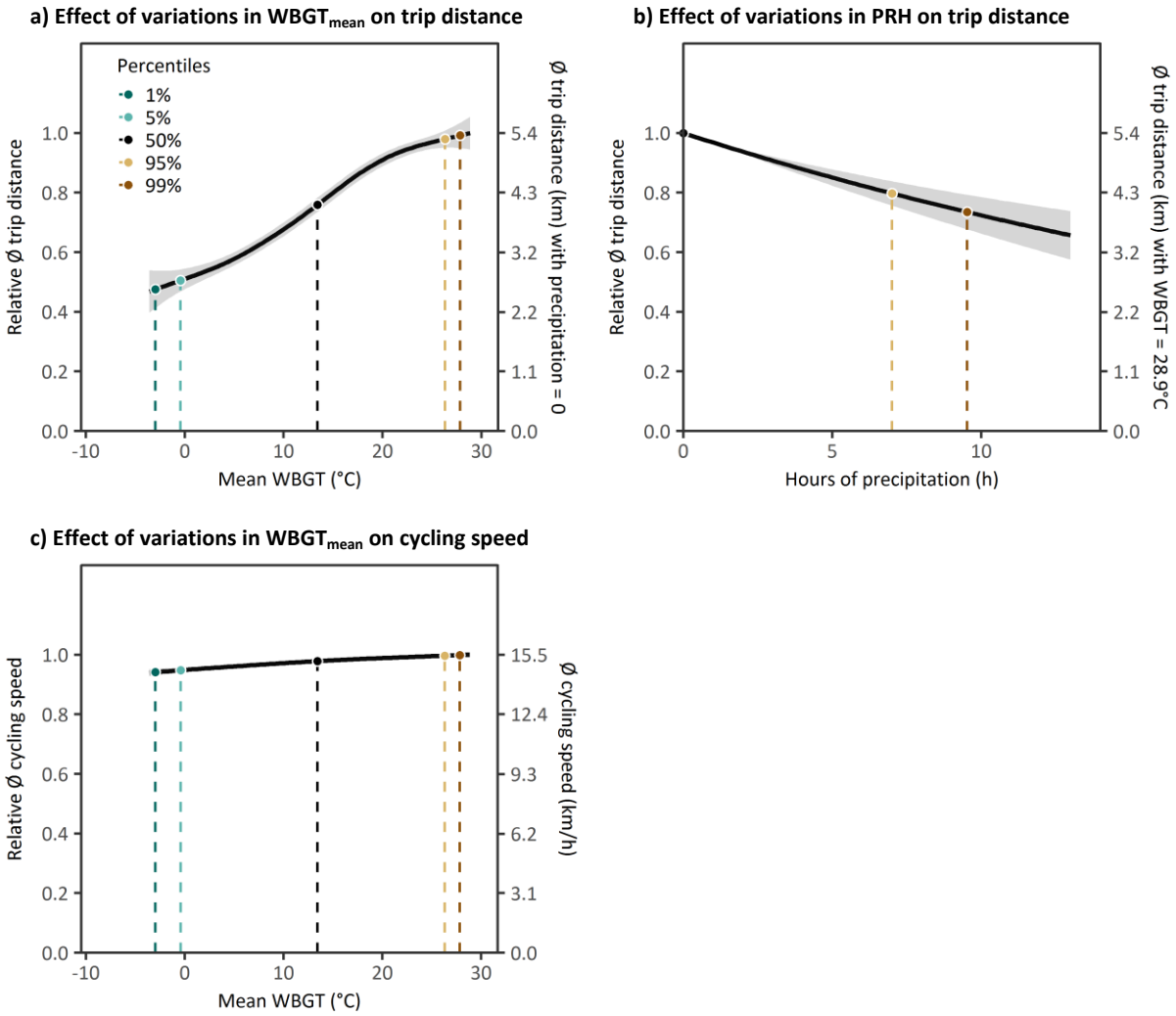

Figure 11: Effect of variations in MET indicators on average trip distance and average cycling speed of tracked trips. Plots refer to workdays only. Period of model calibration: 2016. Plot design based on Marí-Dell'Olmo et al. (2018).

Cycling speed is much less influenced by variations in meteorological conditions than trip distance. Although variations in mean WBGT show a statistically significant effect on average cycling speed, the response is rather small and negligible (see Figure 11.c).

4.3 Effect of meteorological conditions on the spatial distribution of cyclists

The results in chapter 4.1 show the sensitivity of the city's daily BTV towards meteorological conditions on an aggregate – more or less city-wide – level. This section, by contrast, illustrates whether there are spatial differences in how sensitively the city's daily BTV responds to variations in meteorological conditions. In this spatial analysis, BTV is measured in terms of tracked trips. Note that in the prototype version of the *Active Mobility Service* analyses based on tracked trips are limited to the year 2016 (see chapters 1.2 and 2.1). The spatial analysis is done based on raster cells of 2 km squared, as the amount of trips tracked in 2016 does not allow for meaningful analyses at higher resolution. Moreover, only those raster cells are considered that show at least 10 tracks going through them on summer days without rain.

PUCS has received funding from the European Union's Horizon 2020 Research and Innovation Programme under Grant Agreement No. 730004

The remaining raster cells are excluded from the analysis due to too low amounts of tracks (for further technical details see chapter 6.2). Figure 12.a gives an overview on the average daily tracked trips that went through each of the considered raster cells in 2016.

Figure 12.b shows the sensitivity of daily BTV towards variations in meteorological conditions per analysed raster cell. The sensitivity per cell is measured in relation to the city-wide average as derived from the statistical model in chapter 4.1. That is, a value exceeding 1 indicates the cell's sensitivity to be above the city-wide average whereas a value smaller than 1 indicates the cell's sensitivity to be below the city-wide average. As shown in the figure, the sensitivity of daily BTV towards variations in meteorological conditions varies over the city. In the inner parts daily BTV responds less sensitively to variations in meteorological conditions than in the outer parts.

a) Average daily tracked trips ("visits" per cell) **b) Sensitivity towards MET conditions per cell**

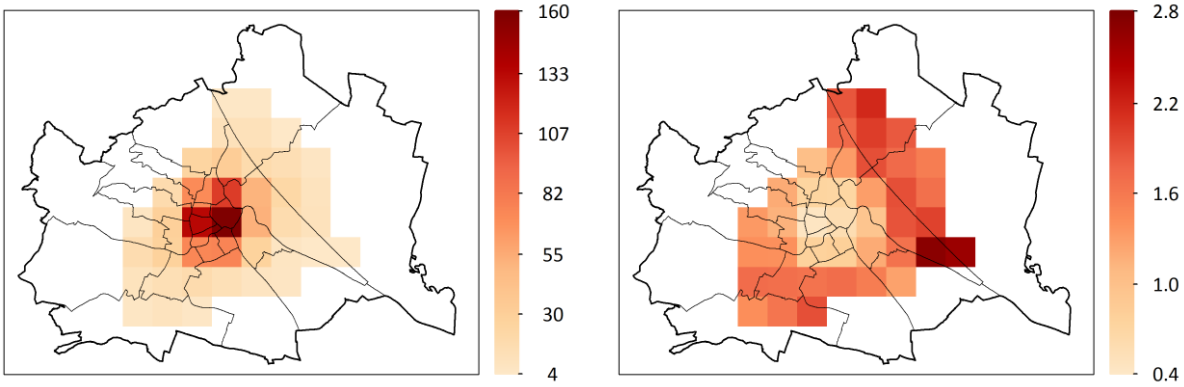

Figure 12: Average daily tracked trips per cell (a) and sensitivity of tracked trips towards variations in MET conditions on workdays (b). The sensitivity per cell is measured relative to the city-wide sensitivity.

Reasons for spatial differences in the meteorological sensitivity of daily BTV may include, amongst others, spatial differences in (i) the bicycle infrastructure (number of cycle paths, number of (roofed) bicycle parking areas, frequency of snow removal of cycling paths, etc.), (ii) the demographic, socioeconomic and psychographic characteristics of the residents (age, sex, family status, attitude, etc.), (iii) the scale of structures (small-scale structures with shorter distances increase the probability for taking the bike despite suboptimal meteorological conditions), (iv) etc.

Using the *Bike Citizens Analytics* tool, further interactive visual in-depth analyses regarding the effects of meteorological conditions on bicycle traffic can be performed. The tool visualizes trips tracked by the *Bike Citizens App* and allows comparing the cycling intensity per stretch of road, based on meteorological conditions. Predefined filters are available for the parameters wet-bulb globe temperature ($WBGT_{mean}$), wind speed (WS_{max}), precipitation (*PRH*), and snow depth (*SD*). Using these filters, workdays characterized by particular meteorological conditions can be selected and the corresponding cycling intensities compared to each other.

By way of example, Figure 13 shows a comparison of the relative cycling intensities on "*usual*" workdays and "*wet*" workdays, where the latter includes workdays with at least five hours of precipitation during daytime. The illustrated map section represents the city centre of Vienna with the Danube in the upper right corner. Cycling intensities are illustrated by the thickness of the streets. Stretches of roads entirely yellow indicate that there is no difference between the relative cycling intensity on "*usual*" and "*wet*" workdays. Red and blue wrappings, by contrast, indicate shifts in the relative cycling intensities when

PUCS has received funding from the European Union's Horizon 2020 Research and Innovation Programme under Grant Agreement No. 730004

comparing "*usual*" and "wet" workdays. The thicker the wrapping, the more pronounced is the shift. Stretches of roads with a blue wrapping show a higher relative cycling intensity on "*wet*" workdays than on "*usual*" workdays. A red wrapping, by contrast, indicates a higher relative cycling intensity on "*usual*" workdays than on "*wet*" workdays. In other words: bluely wrapped roads are over-proportionally used on "*wet*" workdays, whereas redly wrapped roads are under-proportionally used on "*wet*" workdays.

As indicated by Figure 13, many streets in the inner-city are gaining in relative importance on "*wet*" workdays. Potential reasons may include a higher share of short trip distances and a stronger feeling of perceived safety. Approach roads to and streets through open-air leisure facilities (e.g. the Danube Island, the Prater, etc.) are, by contrast, losing relative importance on "*wet*" workdays.

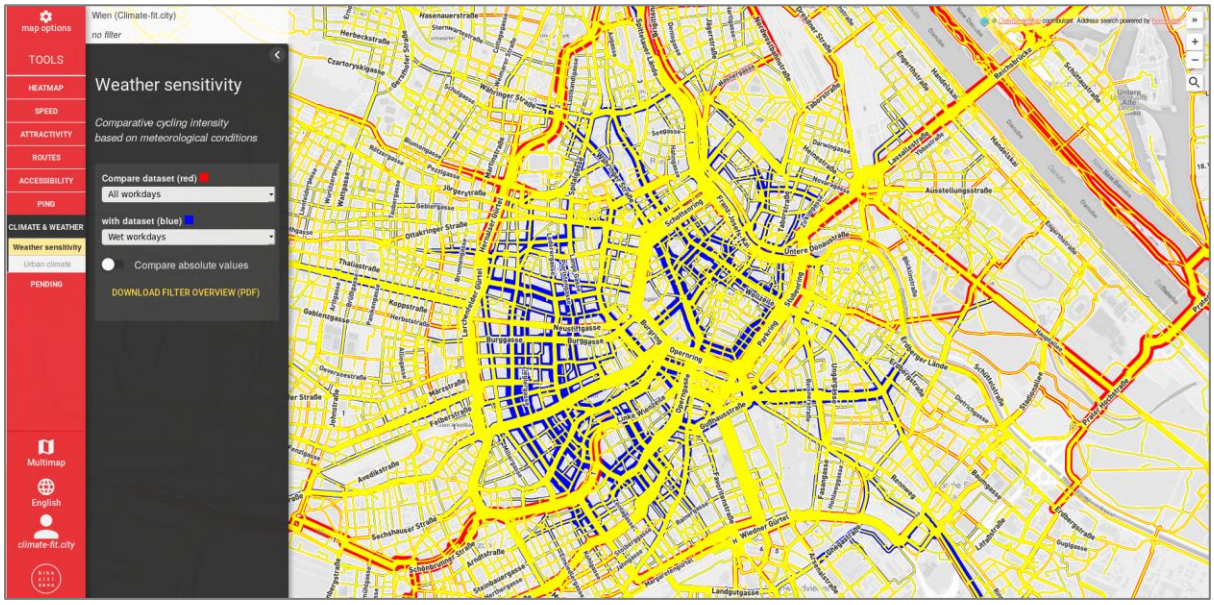

Figure 13: Comparison of relative cycling intensities on usual workdays (red) and "wet" workdays (blue), i.e. workdays with at least five hours of precipitation during daytime (06:00-20:00). Screenshot of Bike Citizens Analytics with zoom into the city centre.

5 The city's climatic attractiveness for cycling

The *Active Mobility Service* assesses a city's climatic attractiveness for cycling from two different perspectives: a rather *objective* one and a more *subjective* one. The *objective* perspective on the city's climatic attractiveness for cycling consists of information derived from climate data only. This includes various evaluations of cycling-relevant meteorological indicators under current and future climatic conditions. The *subjective* perspective, by contrast, describes the city's climatic attractiveness as *perceived* by its cyclists. It is derived by merging climate data with the response functions calculated in chapter 4.1. Whereas *objective* climatic attractiveness is displayed in the original units of measurement of the considered meteorological indicators (e.g. °C, km/h), *subjective* or *perceived* climatic attractiveness is measured in terms of *relative BTV* (see chapter 5.2 for further details). Both, *objective* and *perceived* climatic attractiveness are assessed under current and future climatic conditions, where the latter refers to the period 2036-2065. Climate projections for two different Representative Concentration Pathways (RCPs) are considered, i.e. RCP4.5 (moderate emissions) and RCP8.5 (high emissions) (see chapter 2.2).

PUCS has received funding from the European Union's Horizon 2020 Research and Innovation Programme under Grant Agreement No. 730004

The reason for providing two different measures of climatic attractiveness is to allow for better comparability between cities. Since the sensitivity of BTV to variations in meteorological conditions is supposed to differ across cities, the *perceived* climatic attractiveness will not only display differences in the cities' climates but also differences in how sensitively the cities' cyclists respond to variations in meteorological conditions. Hence, a comparably low *perceived* climatic attractiveness of a city may either result from a high frequency of unfavourable meteorological conditions or from a high sensitivity of the city's BTV to variations in meteorological conditions (or a combination of both). The *Active Mobility Service* allows for differentiating between these two effects by providing information on both, the city's *objective* and *perceived* climatic attractiveness.

5.1 "Objective" climatic attractiveness today and in future

Figure 13 presents evaluations of the meteorological indicators, whose effect on the city's daily BTV was illustrated in chapter 4.1. This includes the mean wet-bulb globe temperature in °C between 06:00 and 20:00 ($WBGT_{mean}$), the maximum mean hourly wind speeds in km/h between 06:00 and 20:00 (WS_{max}), the number of hours with precipitation > 0.1 mm between 06:00 and 20:00 (PRH) and snow depth in cm at 07:00 (SD). In case of $WBGT_{mean}$ and WS_{max}, which both present *UrbClim* outputs, cycling-weighted city-wide averages are used for the analyses. Apart from snow depth, evaluations are presented for both, current and future climatic conditions. For snow depth, no climate projections are available within this prototype version of the *Active Mobility Service*. Thus, evaluations only refer to current climatic conditions.

Plot (a) displays the annual cycle – i.e. monthly averages – of $WBGT_{mean}$ under current and future climatic conditions. January usually shows the lowest, July by contrast the highest values of $WBGT_{mean}$. Under current climatic conditions the monthly averages range from 1.1 °C to 24.1 °C. Due to climate change, the annual average of $WBGT_{mean}$ is projected to rise from 13.0 °C to 15.0 °C (RCP4.5) and 15.5 °C (RCP8.5), respectively. On a monthly basis the highest increases are expected for August and September, the lowest for April and May. This overall warming trend is also reflected in the frequency of cold and hot days. Whereas the number of days per year with $WBGT_{mean}$ below or equal 0 °C is projected to decrease noticeably, the number of days per year with $WBGT_{mean}$ equal or above 30 °C is expected to increase sharply (Figure 13.b).

Besides $WBGT_{mean}$, the number of days with high wind speeds is as well projected to increase in future (Figure 13.e). The same holds true for the average daily number of hours with precipitation during daytime and the average annual number of days with several precipitation hours, i.e. PRH ≥ 5 and PRH ≥ 10 (Figure 13.c and Figure 13.d). However, days with precipitation in general (PRH ≥ 1) are basically projected to decrease slightly (see Figure 13.d). As already mentioned, the prototype version of the *Active Mobility Service* does not include future projections on snow depth. Under current conditions, 28 days with a snow depth of at least 1 cm are on average observed per year (Figure 13.f). Year-to-year variability is, however, high, with the annual number of days with a snow depth of at least 1 cm ranging between 10 and 79.

PUCS has received funding from the European Union's Horizon 2020 Research and Innovation Programme under Grant Agreement No. 730004

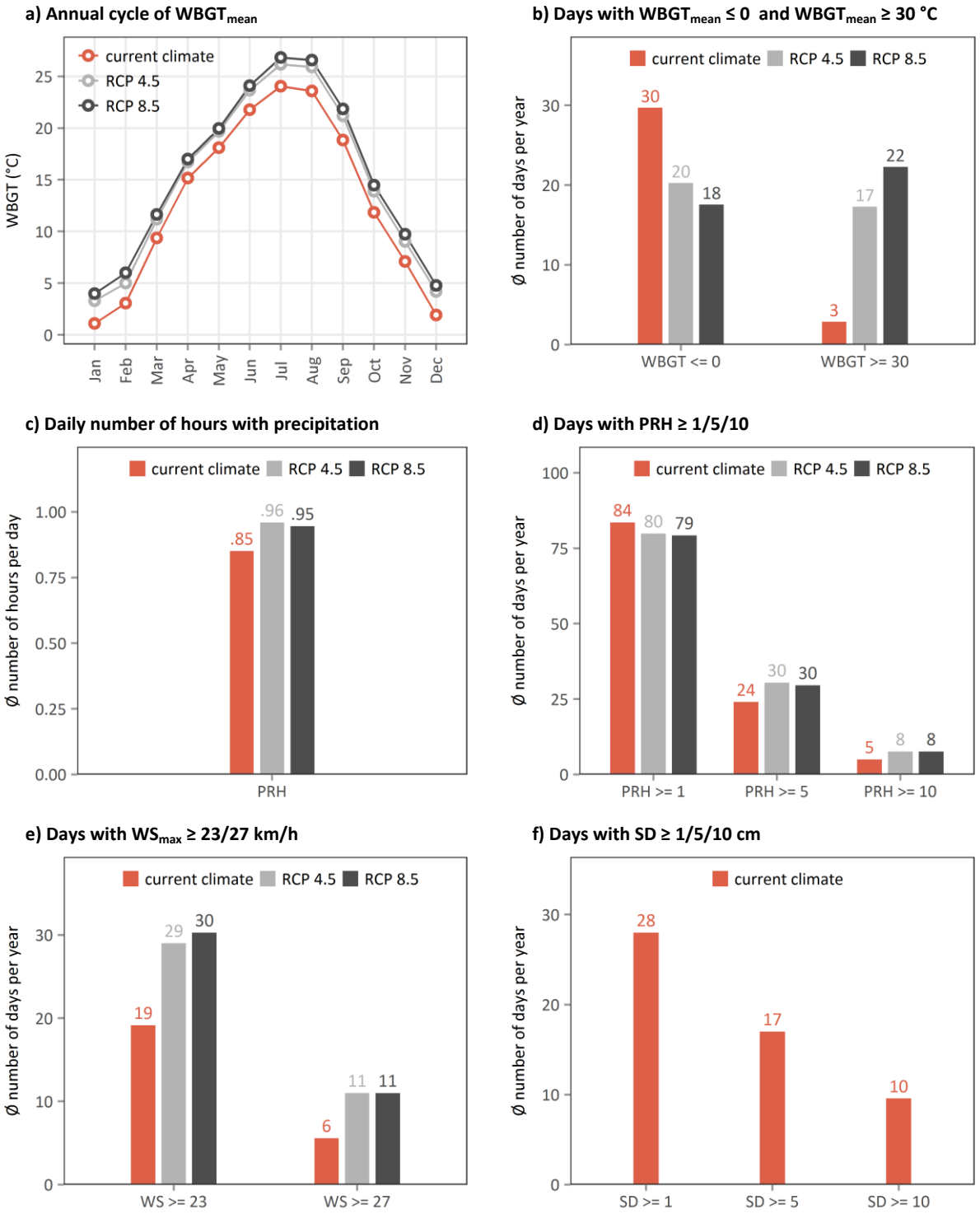

Figure 14: Analyses of the MET indicators WBGT$_{mean}$, PRH, WS$_{max}$, and SD under current and future (Ø 2036-2065) climatic conditions. a) Annual cycle of WBGT$_{mean}$. b) Average annual number of days with WBGT$_{mean}$ ≤ 0 °C and with WBGT$_{mean}$ ≥ 30 °C. c) Average daily number of hours with precipitation. d) Average annual number of days with PRH ≥ 1, PRH ≥ 5 and PRH ≥ 10. e) Average number of days with wind speeds ≥ 23 km/h and wind speeds ≥ 27 km/h. f) Average number of days with snow depth ≥ 1 cm, snow depth ≥ 5 cm and snow depth ≥ 10 cm (only for current climatic conditions).

PUCS has received funding from the European Union's Horizon 2020 Research and Innovation Programme under Grant Agreement No. 730004

Figure 14 provides detailed information on the typical spatial distribution of heat stress on hot days under current and future climatic conditions. It shows the indicator $WBGT_{mean}$ on a 100 m resolution, averaged over all days with a cycling-weighted city-wide $WBGT_{mean}$ of at least 30 °C. The plots allow identifying those regions of the city with the highest exposure to heat stress on hot days. They are also available as selectable layers within *Bike Citizens Analytics*.

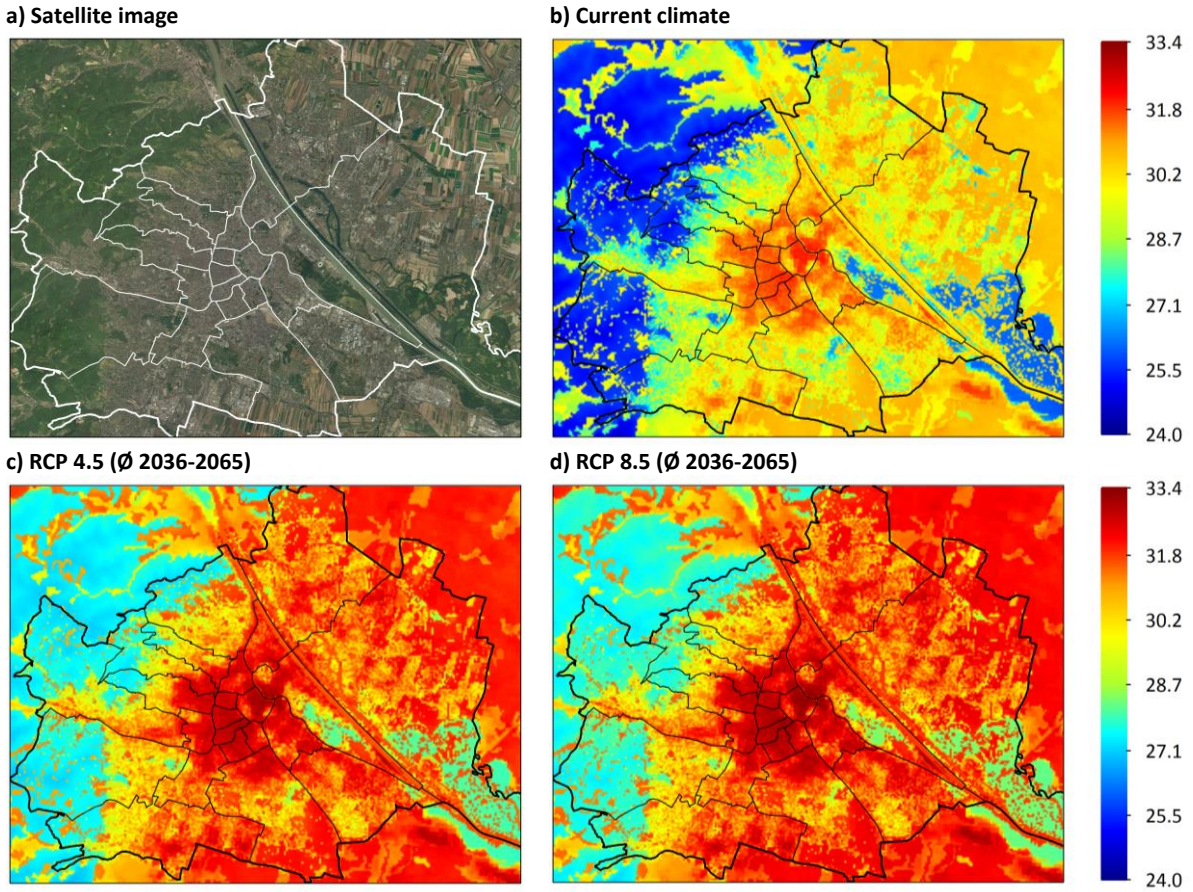

Figure 15: Typical heat stress on hot days under current and future climatic conditions (in °C); i.e. $WBGT_{mean}$ averaged over days with cycling-weighted city-wide $WBGT_{mean} \geq 30$ °C (corresponds to the 99th percentile under current climatic conditions). Resolution: 100 m. Data sources: WBGT data from UrbClim, satellite image from OpenStreetMap, administrative borders from Statistics Austria.

Figure 15 to Figure 18 once again show the typical spatial distribution of heat stress on hot days under current and future climatic conditions, but zooming into particular regions of the city. In addition, roads open to bikers are displayed by black lines in order to allow identifying those (stretches of) roads that are most prone to heat stress on hot days.

Figure 19 provides further information on spatial differences in the exposure to heat stress. It shows the average annual number of days with a mean wet-bulb globe temperature during daytime (i.e. between 06:00 and 20:00) of at least 30 °C at a 100 m resolution. Thus, it adds spatial detail to the information provided by the bars on the right side of Figure 13.b. Again, the information is shown for current as well as future climatic conditions.

PUCS has received funding from the European Union's Horizon 2020 Research and Innovation Programme under Grant Agreement No. 730004

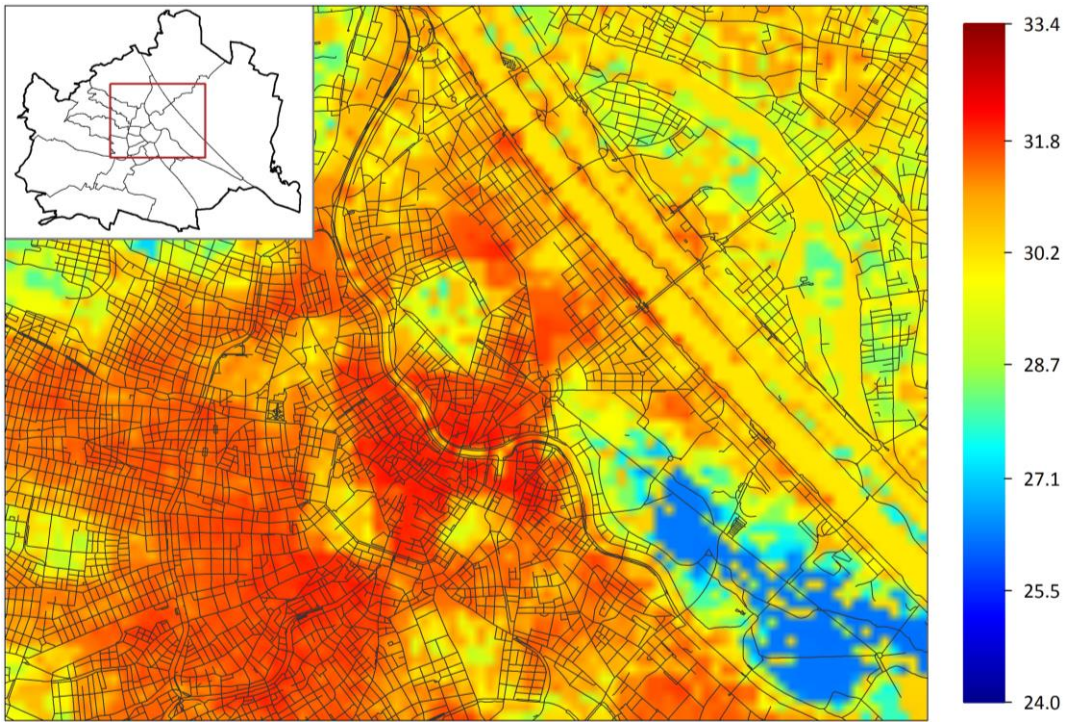

Figure 16: Typical heat stress on hot days under current climatic conditions (in °C); i.e. $WBGT_{mean}$ averaged over days with cycling-weighted city-wide $WBGT_{mean} \geq 30$ °C (corresponds to the 99th percentile). Resolution: 100 m. Zoom into the city's centre. Black lines indicate roads open to bikers. Data sources: WBGT data from UrbClim, roads from gip.gv.at (version 2017-08), administrative borders from Statistics Austria.

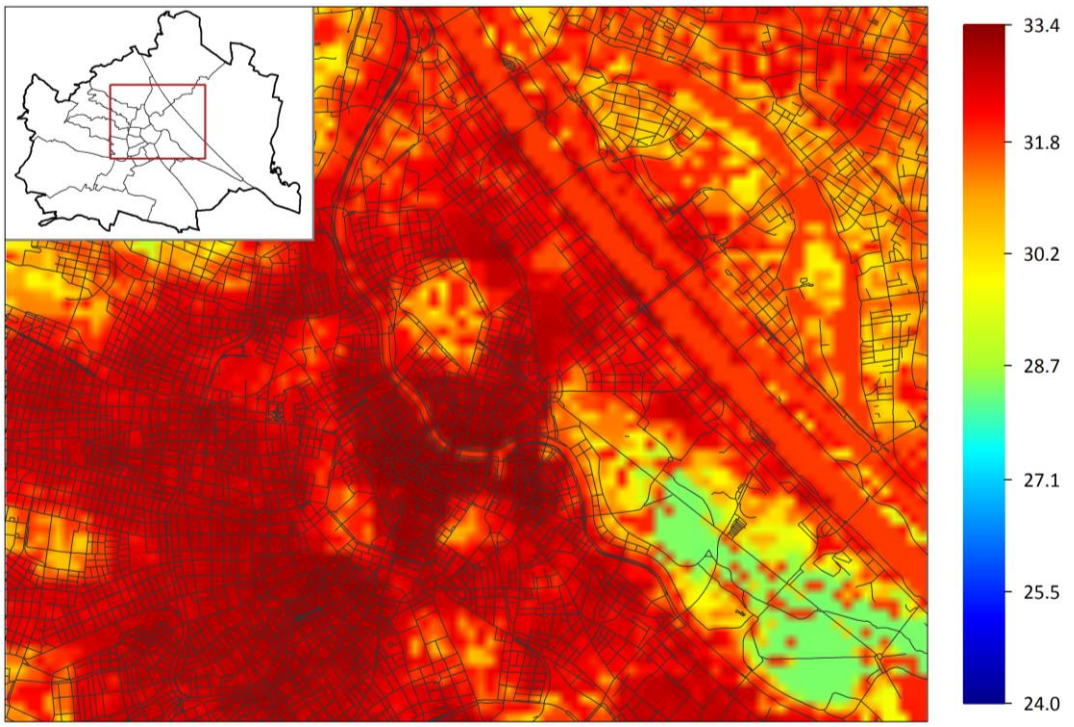

Figure 17: Typical heat stress on hot days under future (Ø 2036-2065; RCP8.5) climatic conditions (in °C); i.e. $WBGT_{mean}$ averaged over days with cycling-weighted city-wide $WBGT_{mean} \geq 30$ °C (corresponds to the 99th percentile). Resolution: 100 m. Zoom into the city's centre. Black lines indicate roads open to bikers. Data sources: WBGT data from UrbClim, roads from gip.gv.at (version 2017-08), administrative borders from Statistics Austria.

PUCS has received funding from the European Union's Horizon 2020 Research and Innovation Programme under Grant Agreement No. 730004

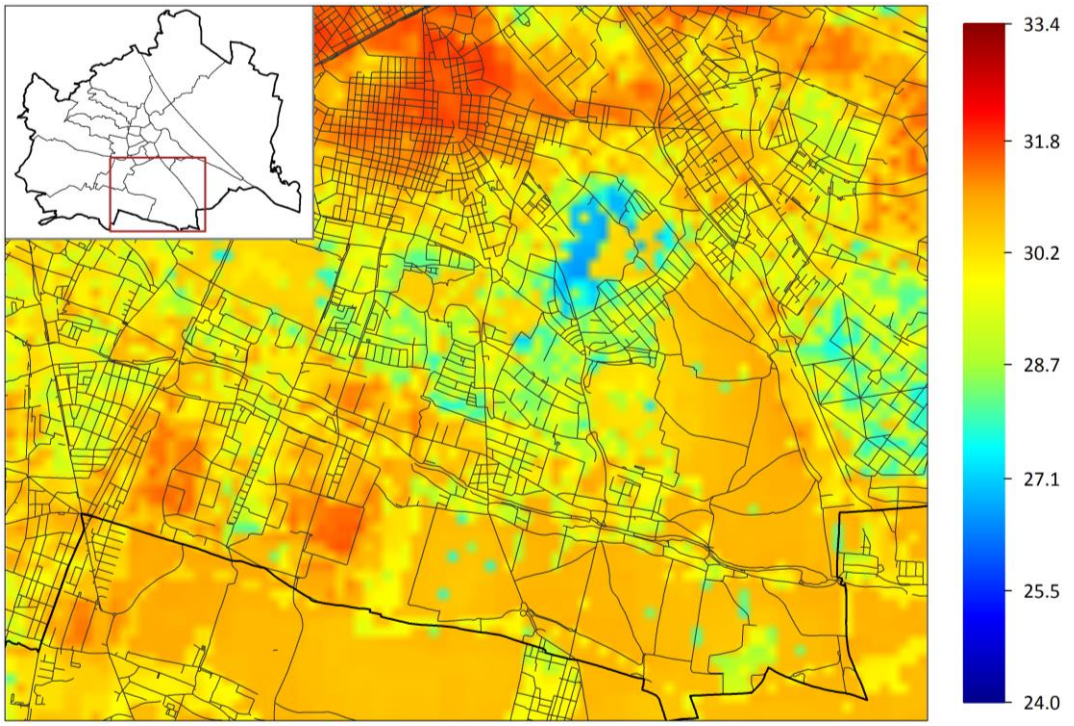

Figure 18: Typical heat stress on hot days under current climatic conditions (in °C); i.e. $WBGT_{mean}$ averaged over days with cycling-weighted city-wide $WBGT_{mean} \geq 30$ °C (corresponds to the 99th percentile). Resolution: 100 m. Zoom into the city's south. Black lines indicate roads open to bikers. Data sources: WBGT data from UrbClim, roads from gip.gv.at (version 2017-08), administrative borders from Statistics Austria.

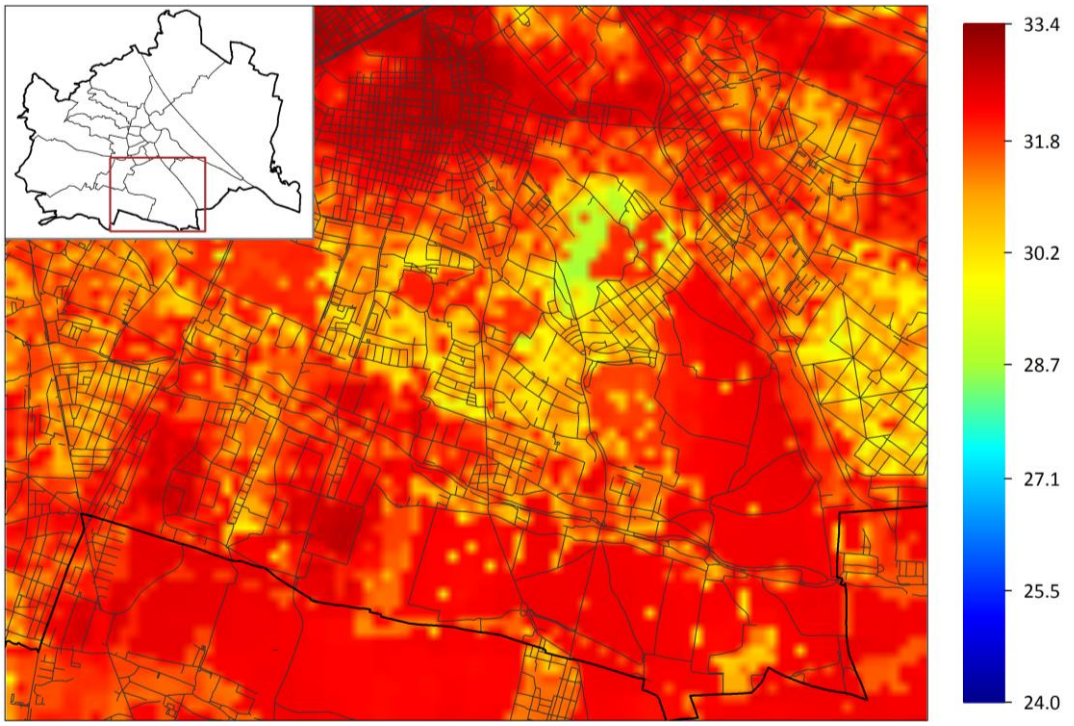

Figure 19: Typical heat stress on hot days under future (Ø 2036-2065; RCP8.5) climatic conditions (in °C); i.e. $WBGT_{mean}$ averaged over days with cycling-weighted city-wide $WBGT_{mean} \geq 30$ °C (corresponds to the 99th percentile). Resolution: 100 m. Zoom into the city's south. Black lines indicate roads open to bikers. Data sources: WBGT data from UrbClim, roads from gip.gv.at (version 2017-08), administrative borders from Statistics Austria.

PUCS has received funding from the European Union's Horizon 2020 Research and Innovation Programme under Grant Agreement No. 730004

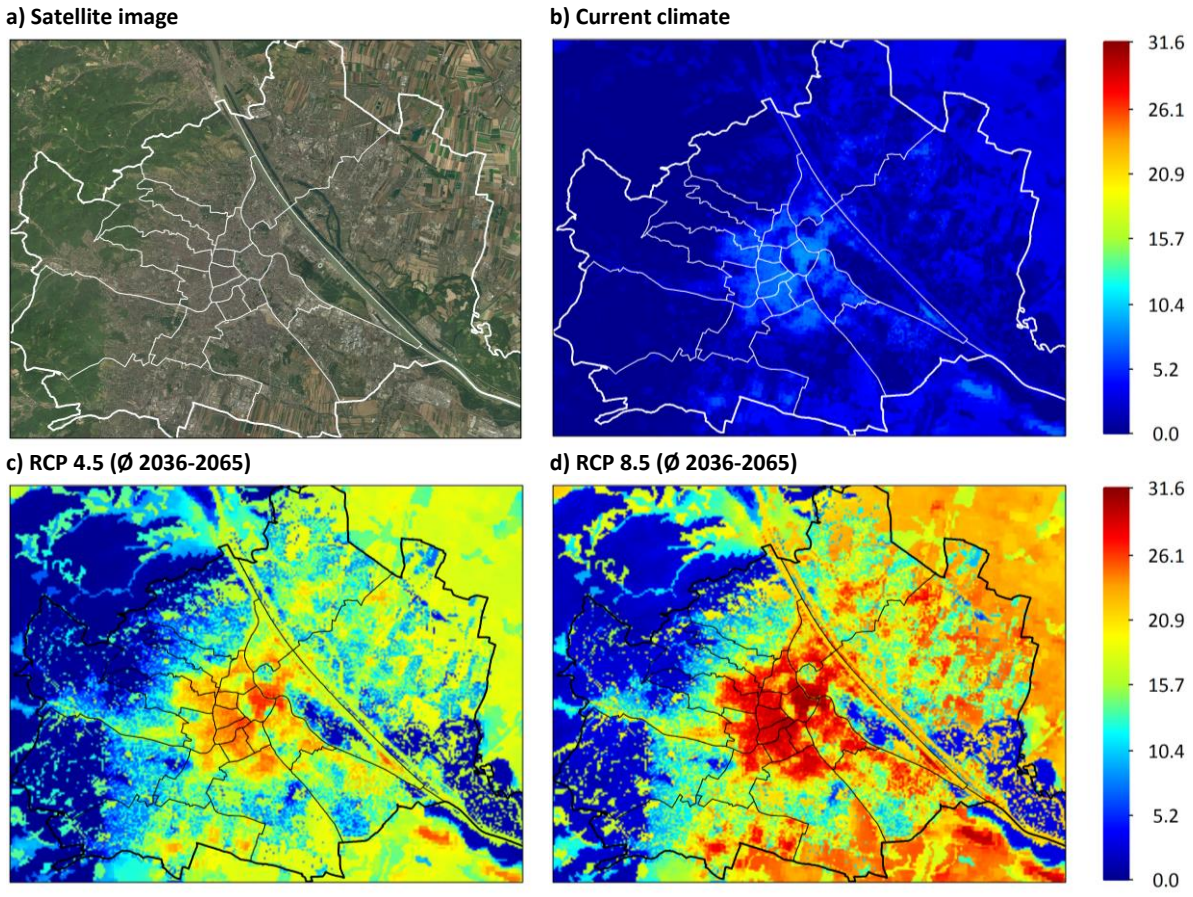

Figure 20: Average annual number of days with $WBGT_{mean} \geq 30$ °C under current and future climatic conditions (in °C). Resolution: 100 m. Data sources: WBGT data from UrbClim, satellite image from OpenStreetMap, administrative borders from Statistics Austria.

Figure 20 to Figure 23 once again show the average annual number of days with a mean wet-bulb globe temperature during daytime of at least 30 °C under current and future climatic conditions, but zooming into the centre of the city. Note that Figure 20 and Figure 21 both display the same data, i.e. the number of days with mean WBGT during daytime of at least 30 °C under current climatic conditions, but use a different colour scaling. In Figure 20, the applied colour scaling is adjusted to the range of values observed under current climatic conditions and thus allows for a better discriminability of spatial differences. Figure 21, by contrast, uses the same uniform colour scaling as applied in Figure 19, Figure 22 and Figure 23. This colour scaling covers the whole range of values under current and future climatic conditions and allows for easy visual comparability of different time periods.

In addition to the spatial details on heat stress, Figure 24 and Figure 25 provide information on the typical spatial distribution of wind speeds on stormy days for particular regions of the city. They show the indicator WS_{max} on a 100 m resolution, averaged over all days with a cycling-weighted city-wide WS_{max} of at least 27 km/h. Both figures refer to current climatic conditions. In addition to the distribution of wind speeds, roads open to bikers are again displayed by black lines.

PUCS has received funding from the European Union's Horizon 2020 Research and Innovation Programme under Grant Agreement No. 730004

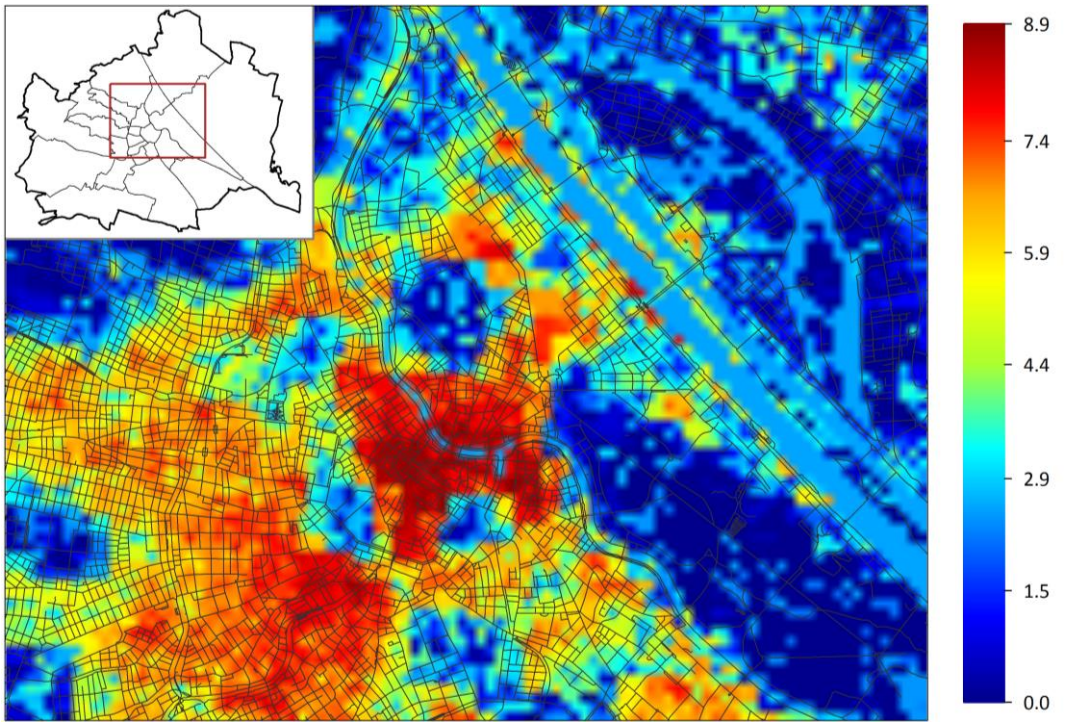

Figure 21: Average annual number of days with $WBGT_{mean} \geq 30$ °C under current climatic conditions. Note: for a better discriminability of spatial differences, the colour scaling differs from Figure 19. Resolution: 100 m. Zoom into the city's centre. Black lines indicate roads open to bikers. Data sources: WBGT data from UrbClim, roads from gip.gv.at (version 2017-08), administrative borders from Statistics Austria.

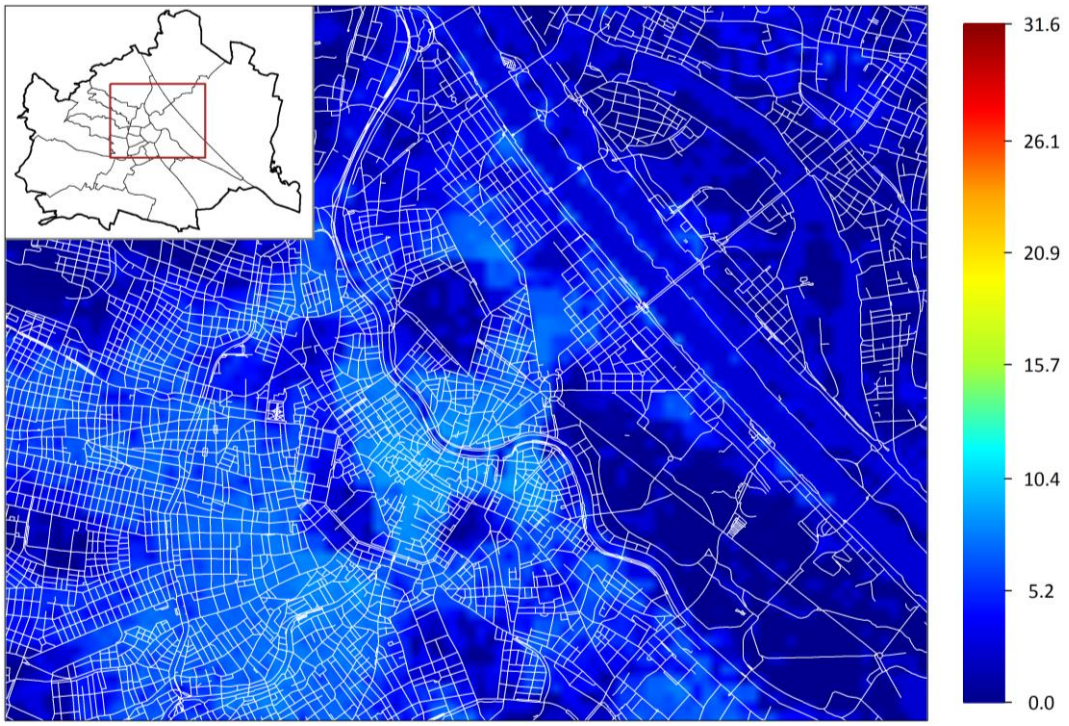

Figure 22: Average annual number of days with $WBGT_{mean} \geq 30$ °C under current climatic conditions. Note: the same colour scaling as in Figure 19 is used. Resolution: 100 m. Zoom into the city's centre. White lines indicate roads open to bikers. Data sources: WBGT data from UrbClim, roads from gip.gv.at (version 2017-08), administrative borders from Statistics Austria.

PUCS has received funding from the European Union's Horizon 2020 Research and Innovation Programme under Grant Agreement No. 730004

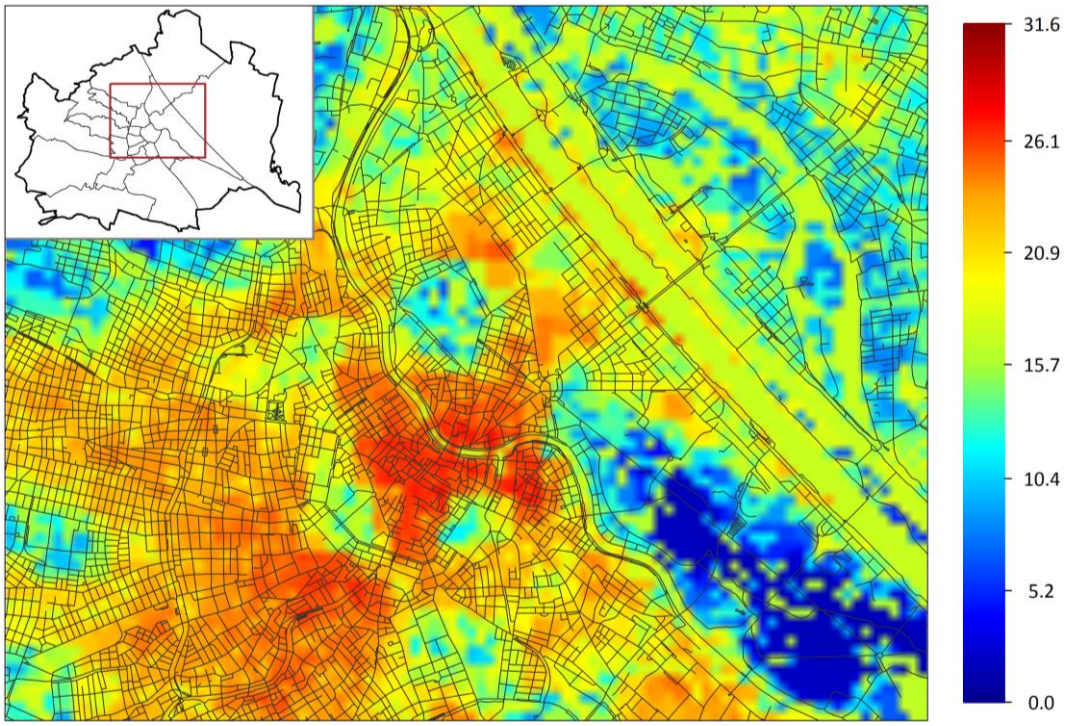

Figure 23: Average annual number of days with $WBGT_{mean} \geq 30$ °C under future climatic conditions (Ø 2036-2065; RCP4.5). Resolution: 100 m. Zoom into the city's centre. Black lines indicate roads open to bikers. Data sources: WBGT data from UrbClim, roads from gip.gv.at (version 2017-08), administrative borders from Statistics Austria.

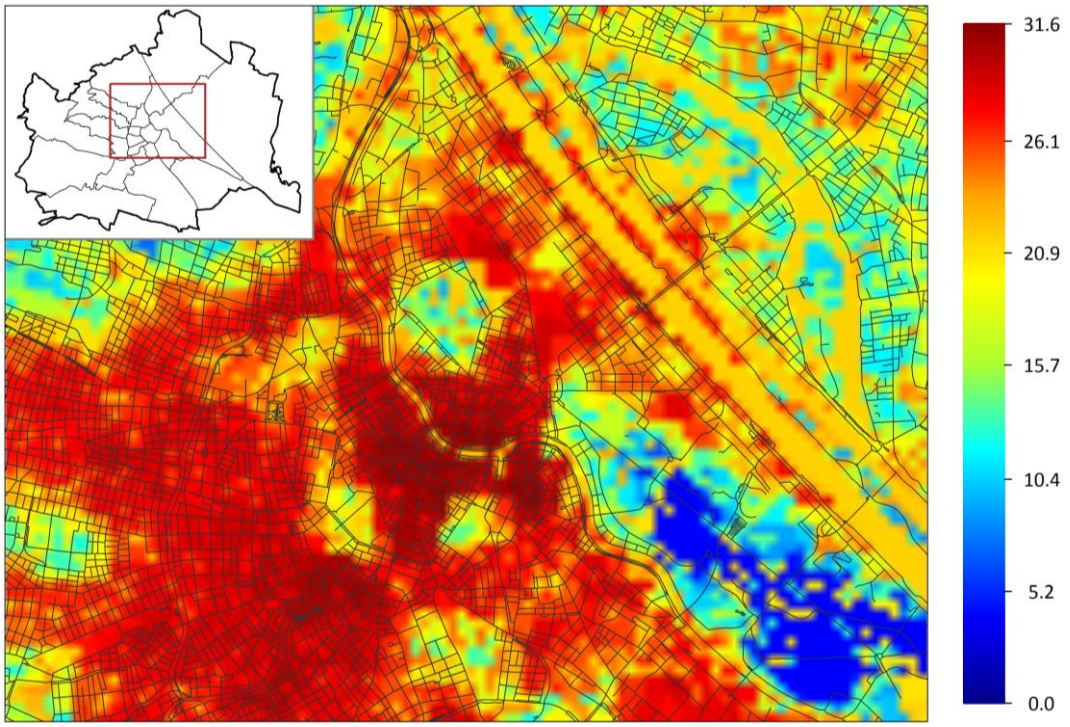

Figure 24: Average annual number of days with $WBGT_{mean} \geq 30$ °C under future climatic conditions (Ø 2036-2065; RCP8.5). Resolution: 100 m. Zoom into the city's centre. Black lines indicate roads open to bikers. Data sources: WBGT data from UrbClim, roads from gip.gv.at (version 2017-08), administrative borders from Statistics Austria.

PUCS has received funding from the European Union's Horizon 2020 Research and Innovation Programme under Grant Agreement No. 730004

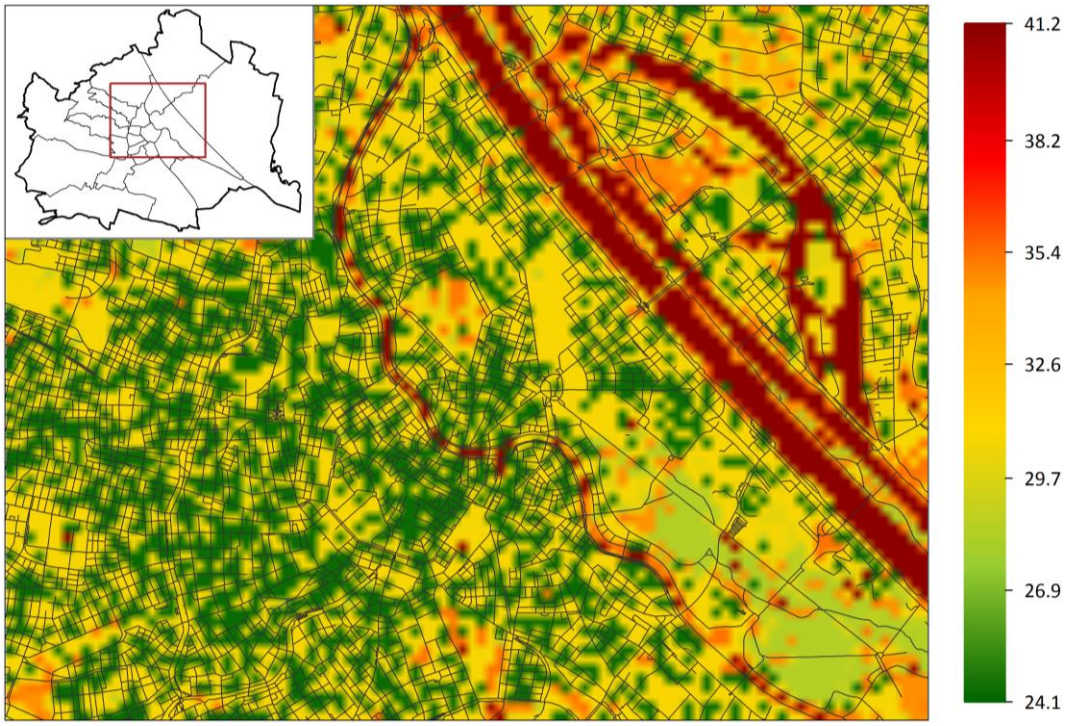

Figure 25: Typical wind speeds on particularly windy days under current climatic conditions (in km/h); i.e. WS_{max} averaged over days with cycling-weighted city-wide $WS_{max} \geq 27$ km/h (corresponds to the 99th percentile). Resolution: 100 m. Zoom into the city's centre. Black lines indicate roads open to bikers. Data sources: wind data from UrbClim, roads from gip.gv.at (version 2017-08), administrative borders from Statistics Austria.

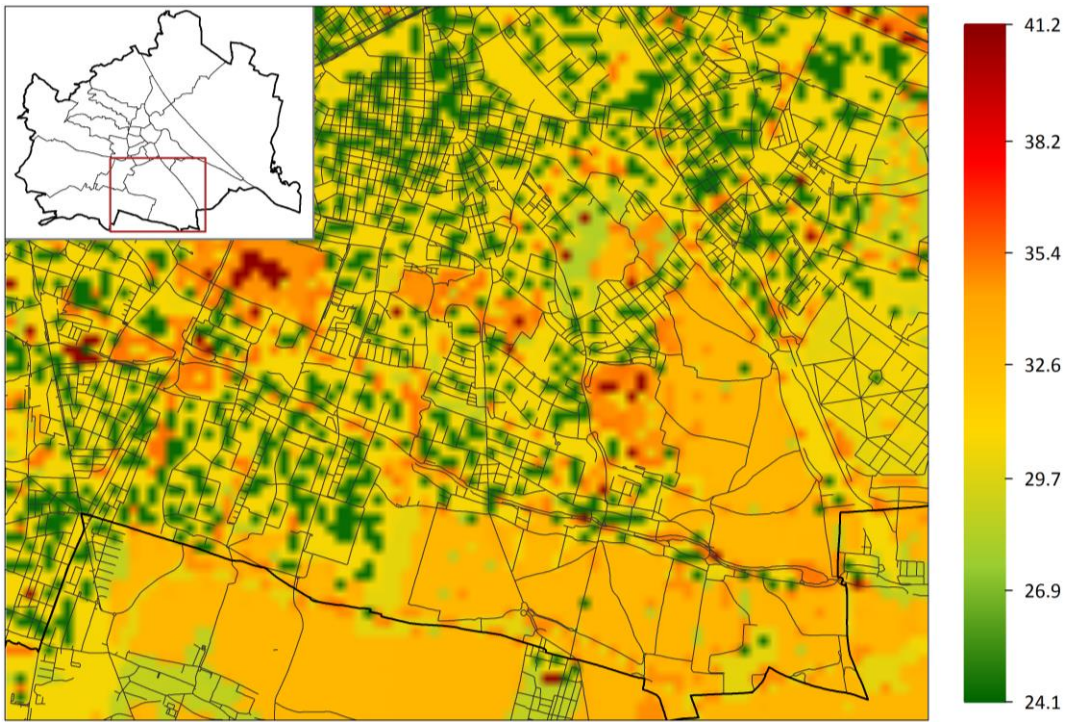

Figure 26: Typical wind speeds on particularly windy days under current climatic conditions (in km/h); i.e. WS_{max} averaged over days with cycling-weighted city-wide $WS_{max} \geq 27$ km/h (corresponds to the 99th percentile). Resolution: 100 m. Zoom into the city's south. Black lines indicate roads open to bikers. Data sources: Wind data from UrbClim, roads from gip.gv.at (version 2017-08), administrative borders from Statistics Austria.

PUCS has received funding from the European Union's Horizon 2020 Research and Innovation Programme under Grant Agreement No. 730004

Cycling-tailored urban climate data, as presented in Figure 15 to Figure 26, can also be accessed via *Bike Citizens Analytics*. With its split-screen function, the tool allows for a visual comparison of urban climate data and cycling intensities. An example of this split-screen function is illustrated in Figure 27. The left screen in Figure 27 shows the typical spatial distribution of thermal comfort under current climatic conditions for the city centre of Vienna. Thermal comfort is represented by the mean wet-bulb globe temperature during daytime (06:00-20:00). The right screen visualizes the typical distribution of cycling intensities based on the trips tracked by the *Bike Citizens App*. This kind of information can support the identification of regions with priority needs for adaptation measures (i.e. regions that are both, heavily frequented by cyclists and frequently exposed to unfavourable climatic conditions).

Figure 27: Example of the split-screen function within Bike Citizens Analytics. Left screen: typical distribution of thermal comfort under current climatic conditions on 100 m resolution (i.e. $WBGT_{mean}$ on an average day). Right screen: typical distribution of cycling intensities based on the trips tracked by the Bike Citizens App. Zoom into the city's centre.

The split-screen function within *Bike Citizens Analytics* can also be used to visualize cycling-tailored urban climate data together with the comparison of relative cycling intensities under different meteorological conditions. Figure 28 provides an example for such a simultaneous visualization. The left screen in Figure 28 again illustrates the typical distribution of thermal comfort under current climatic conditions for the city centre of Vienna. The right screen shows a comparison of the relative cycling intensities on "*usual*" workdays and "*hot*" workdays, where the latter includes workdays with a cycling-weighted city-wide mean wet-bulb globe temperature of at least 30 °C during daytime. Stretches of roads with a blue wrapping show a higher relative cycling intensity on "*usual*" workdays than on "*hot*" workdays. A red wrapping, by contrast, indicates a higher relative cycling intensity on "*hot*" workdays than on "*usual*" workdays. In other words: redly wrapped roads are over-proportionally used on "*hot*" workdays, whereas bluely wrapped roads are under-proportionally used on "*hot*" workdays.

As displayed in the left screen of Figure 28, regions with comparably high perceived temperatures are particularly located in the middle and the lower left-hand part of the map section shown. Streets in these regions tend to lose relative importance on "*hot*" days, as illustrated by the screen on the right-hand side.

PUCS has received funding from the European Union's Horizon 2020 Research and Innovation Programme under Grant Agreement No. 730004

Approach roads to and streets through cooling open-air leisure facilities (e.g. the Danube Island, the Prater, etc.), by contrast, tend to gain in relative importance on "*hot*" workdays.

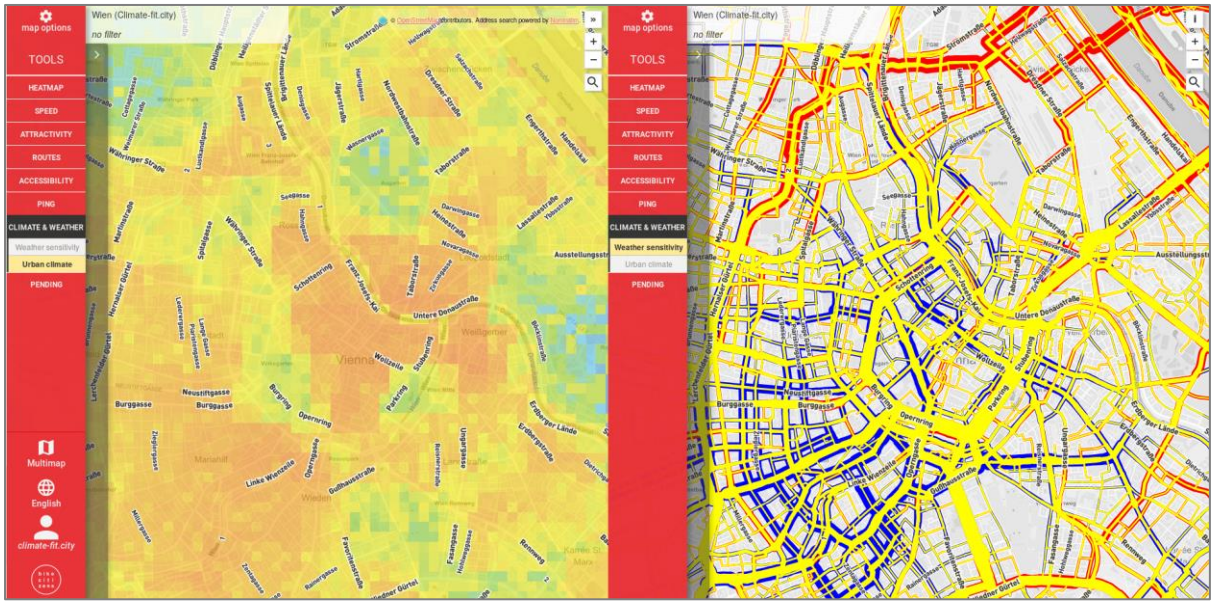

Figure 28: Example of the split-screen function within Bike Citizens Analytics. Left screen: typical distribution of thermal comfort under current climatic conditions on 100 m resolution (i.e. $WBGT_{mean}$ on an average day). Right screen: comparison of relative cycling intensities on usual workdays (blue) and "hot" workdays (red), where "hot" refers to workdays with a cycling-weighted city-wide mean wet-bulb globe temperature of at least 30 °C during daytime (06:00-20:00). Zoom into the city's centre.

5.2 "Subjective" climatic attractiveness today and in future

The *subjective* or *perceived* climatic attractiveness represents the assessment of the city's current and future climatic conditions based on how sensitively the city's cyclists respond to variations in meteorological conditions nowadays (see chapter 4.1)[13]. The *perceived* climatic attractiveness is measured in relative terms. A value of 1 corresponds to the city's BTV that would be expected if meteorological conditions were optimal throughout the year. Figure 26 shows the city's climatic attractiveness as perceived by its cyclists under current (orange-red bars) and future (grey bars) climatic conditions.

Based on their observed cycling habits, cyclists in Vienna assess the city's current climatic attractiveness with a value of about 0.58. Remember that a value of 1 represents the highest possible score. It would result if cyclists perceived the climatic conditions as optimal throughout the whole year or if they were completely insensitive towards variations in meteorological conditions. Vienna's climatic attractiveness, as perceived by its cyclists, varies with the course of the year. Whereas the climatic conditions in January are the least appreciated ones by cyclists in Vienna (0.26), climatic conditions typically experienced in July and August rank among the most valued ones (0.85).

[13] For assessing the perceived climatic attractiveness, we use the sensitivities resulting from measuring BTV in terms of counts at considered counting stations. Due to the longer time period available for model calibration, estimates are more robust than in case of measuring BTV in terms of tracked trips (see chapter 4.1).

PUCS has received funding from the European Union's Horizon 2020 Research and Innovation Programme under Grant Agreement No. 730004

A perceived annual climatic attractiveness of 0.58 indicates that there is a high theoretical potential for substantial increases in bicycle usage by reducing the cyclists' sensitivity towards variations in meteorological conditions. This theoretical potential amounts to an increase in the current average annual bicycle traffic volume by about 70 %.

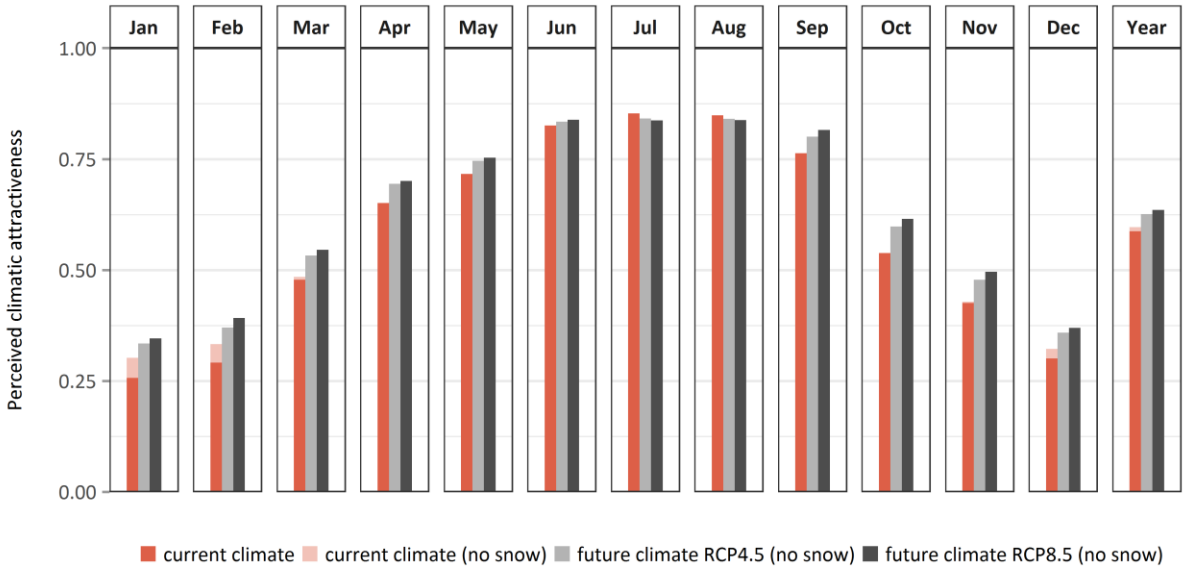

Figure 29: The city's climatic attractiveness as perceived by its cyclists under current and future (Ø 2036-2065) climatic conditions. A value of 1 corresponds to the expected BTV under permanent optimal climatic conditions.

As already mentioned, no projections on snow depth are available for future climatic conditions in this prototype version of the *Active Mobility Service*. Hence, the *perceived* climatic attractiveness under future conditions is assessed without considering the effect of snow on the ground. For reasons of comparability, Figure 26 thus also shows the *perceived* climatic attractiveness under current climatic conditions when assuming no days with snow on the ground. Bars in orange-red show the actual perceived attractiveness of the current climatic conditions whereas bars in bright-red show how attractive climatic conditions would be perceived in case of no days with snow on the ground. Without snow on the ground climatic attractiveness would, for example, be assessed with about 0.30 instead of 0.26 in January.

Vienna's *perceived* climatic attractiveness for cycling is projected to increase in future. This rise in *perceived* climatic attractiveness covers all months apart from July and August, where the expected increase in hot days somewhat mutes *perceived* climate attractiveness (Figure 26). Overall, the expected rise in *perceived* climatic attractiveness is however small compared to the potential for bike usage increases that lies in making cycling less sensitive towards variations in meteorological conditions.

Table 6 gives an overview on the frequency of meteorological conditions that cause the city's daily BTV to drop by a particular percentage when occurring on a workday. This percentage drop is measured compared to the BTV expected under optimal climatic conditions. The frequency of occurrence of such meteorological conditions – measured in days per year – is shown for current as well as future (Ø 2036-2065) climatic conditions. Taking the effect of snow on the ground into account, there are currently about 58 days per year with meteorological conditions that cause the city's BTV to drop by more than 70 % when occurring on a workday (compared to the expected BTV under optimal

PUCS has received funding from the European Union's Horizon 2020 Research and Innovation Programme under Grant Agreement No. 730004

meteorological conditions). Disregarding the effect of snow on the ground, it's only 47 days per year. Under future climatic conditions, this frequency is expected to drop to 37 (RCP 4.5) and 34 (RCP 8.5) days per year, respectively.

Table 6: Frequency of MET conditions causing considerable drops in the city's BTV compared to optimal MET conditions

Change in BTV (compared to optimal MET conditions)	Frequency of occurrence (days/year)			
	Current climatic conditions	Current climatic conditions (no snow)	Future* climatic conditions RCP 4.5 (no snow)	Future* climatic conditions RCP 8.5 (no snow)
> -50 %	~159	~159	~140	~134
> -60 %	~121	~121	~99	~90
> -70 %	~58	~47	~37	~33
> -80 %	~27	~8	~8	~6
> -90 %	~5	~0	~0	~0

*) Future climatic conditions: Ø 2036-2065

PUCS has received funding from the European Union's Horizon 2020 Research and Innovation Programme under Grant Agreement No. 730004

PART C | TECHNICAL DETAILS

6 Methodology

This chapter provides some technical details on the statistical models used in the *Active Mobility Service*. For technical details on the urban climate model *UrbClim,* see De Ridder et al. (2015). Details on the methodology of downscaling climate projections and generating the future climate data used in the *Active Mobility Service* can be found in Lauweat et al. (2018).

6.1 Statistical model: meteorological sensitivity of total bicycle traffic volume

So called generalized additive models (GAM) are used in chapter 4.1 to explain variations in the city's daily BTV and assess its sensitivity towards meteorological conditions. GAMs are generalized linear models in which the regressand – the city's daily BTV in this case – linearly depends on unknown smooth functions of some regressors or explanatory variables. Hence, potential non-linear effects of particular meteorological indicators can be easily considered.

The regressors entering the final model are selected from a larger set of potential regressors by a mixture of automatic algorithm and manual refinement. The compilation of the starting set of potential regressors is based on the literature (Ahmed et al. 2010; Böcker and Thorsson 2014; Brandenburg et al. 2007; El-Assi et al. 2015; Flynn et al. 2012; Helbich et al. 2014; Phung and Rose 2007; Thomas et al. 2013). In the first step of the selection procedure, an automatic algorithm is used to pre-select a reasonable number of regressors out of the starting set. The method starts with an empty model and then iteratively adds new regressors until an abort criterion is fulfilled. In each step the regressor that maximizes the quality of the model, which is estimated using the Generalized Cross Validation (GCV), is added. After a new variable has been added it is tested whether dropping each chosen regressor would improve model quality. The algorithm stops when the improvement in GCV is smaller than a given threshold. Again, it is tested whether exchanging one regressor with another – not yet being in the model – would improve model quality. Following the automatic selection procedure, the model is manually refined. Especially the number of used regressors is reduced and possible shape constraints on the smooth functions are added to find more robust models.

The general model structure looks as follows:

$$\log(BTV) \sim s(MI_1) + s(MI_2) + MI_3 + (MI_4 > a) + C_1 + C_2 + \cdots \qquad \textit{Eq. 1}$$

where BTV is the city's daily bicycle traffic volume, MI_i are different meteorological indices, C_i are other explanatory variables, s denotes a smooth function, and a_i defines a threshold.

The final model used to explain variations in the city's BTV on workdays takes the following form (see Table 3 for a description of the single explanatory variables):

PUCS has received funding from the European Union's Horizon 2020 Research and Innovation Programme under Grant Agreement No. 730004

$$\log(BTV) \sim s(WBGT_{mean}) + s(PRH) + s(WS_{max}) + s(SD) + population + christmas.holidays + easter.holidays + summer.holidays + semester.breaks + weekday + bridging.day + s(day.length) \quad \text{Eq. 2}$$

Note that the statistical model that uses tracked trips as a measure of the city's daily BTV additionally includes a variable accounting for the increase in users of the Bike Citizens App over time. On the other hand, the annual variable *population* is not considered in the model for tracked trips, as only one year (2016) is available for model calibration.

As described in chapter 4.1, data on WBGT and wind speed come from the urban climate model *UrbClim* (driven by ERA5 reanalysis data), whereas data on precipitation and snow depth stem from local measurement stations. As an alternative to local measurement stations, we also could have used ERA5 reanalysis data – available on a 30 km grid – as a source for precipitation and snow depth data. However, measurements from local stations revealed slightly better model performances in this case.

GAMs are also applied for investigating the effect of variations in meteorological conditions on average trip distance and average cycling speed on workdays (see chapter 4.2). In those cases, the final model specifications only include statistically significant meteorological indicators but no calendric or socio-economic parameters as explanatory variables:

$$\log(distance) \sim s(WBGT_{mean}) + s(PRH) \quad \text{Eq. 3}$$

$$\log(speed) \sim s(WBGT_{mean}) \quad \text{Eq. 4}$$

where *distance* is the daily average trip distance and *speed* is the daily average cycling speed.

6.2 Statistical model: spatial characteristics of meteorological sensitivity

As described in chapter 4.3, potential spatial differences in the sensitivity of daily BTV are analysed on a 2 km x 2 km grid and by measuring BTV in terms of tracked trips. The GAM fitted to explain variations in the city-wide daily BTV serves as a starting base. It is used to simulate BTV for each workday in the year 2016 and for each considered grid cell in a first step. These simulations are split into a calendric effect (CE) and a meteorological effect (ME). In a second step we assess how well the city-wide model simulates BTV for each individual cell by fitting the following model:

$$log(BTV_j) \sim \mathrm{CE_j} + \mathrm{ME_j} \quad \text{Eq. 5}$$

where BTV_j denotes cell j's daily bicycle traffic volume measured in terms of the number of tracked trips passing through cell j, CE_j is the calendric effect for cell j as simulated by the city-wide model, and ME_j refers to the meteorological effect for cell j as simulated by the city-wide model. If the coefficients resulting for the calendric effect and the meteorological effect are both 1, the city-wide model fits perfectly for describing BTV in the respective cell. That is, calendric effect and meteorological effect of the respective cell equal the city-wide effects. If, by contrast, the coefficient resulting for the meteorological effect exceeds 1, BTV in the respective cell responds more sensitively to variations in meteorological conditions than city-wide BTV. If the coefficient is below 1, the meteorological sensitivity of BTV in the respective cell lies below the city-wide average.

PUCS has received funding from the European Union's Horizon 2020 Research and Innovation Programme under Grant Agreement No. 730004

7 Supplement: estimating the total number of bicycle trips

In this supplementary section we estimate the total number of bicycle trips on workdays. This is done by extrapolating the data from the automatic counting stations through data on trips tracked by the Bike Citizens App. The applied method assumes that the ratio between the total number of bicycle trips (T_{total}) and the total number of counts at stations (CS_{total}) equals the ratio between the number of tracked trips ($T_{tracked}$) and the number of counts at stations belonging to a tracked trip ($CS_{tracked}$):

$$\frac{T_{total}}{CS_{total}} = \frac{T_{tracked}}{CS_{tracked}} \qquad \textit{Eq. 6}$$

Then, the total number of bicycle trips can be estimated as follows:

$$T_{total} = CS_{total} \times \frac{T_{tracked}}{CS_{tracked}} \qquad \textit{Eq. 7}$$

Calculating the total number of counts at stations (CS_{total}) and the number of tracked trips ($T_{tracked}$) is straightforward. To estimate the number of counts at stations belonging to a tracked trip ($CS_{tracked}$) we assume each tracked trip that passes a counting station within 10 m distance to be counted by this station. This gives us an estimation of how many counts of a station belong to a tracked trip.

Before applying the above equation, the suitability of the chosen method needs to be assessed. Note, that the proposed method only provides meaningful results if both, cyclists counted by the counting stations and cyclists tracking their trips behave more or less in the same way as the whole population of cyclists in Vienna. As we do not have information about the whole population of cyclists in Vienna, we cannot compare their behaviour to that of cyclists counted by the counting stations and of cyclists tracking their trips. What we can do, however, is to compare the latter two to each other.

As illustrated in Eq. 7, the chosen method assumes a linear relationship between CS_{total} and $CS_{tracked}$ as well as between $T_{tracked}$ and $CS_{tracked}$. To check, whether the first of these two assumptions empirically more or less holds, Figure 27 gives a visual illustration of the relationship between total daily counts per counting station (CS_{total}) and daily counts of tracked trips per counting station ($CS_{tracked}$). At counting stations with a high number of tracked trips, this relationship turns out to be more or less linear. In other words, there tends to be a good correspondence between total counts and counts of tracked trips at those stations that are frequently passed by cyclists tracking their trips. In a second step, we estimate a linear model for each station that explains the daily total counts by the daily counts of tracked trips. Figure 28 shows the multiplication factors resulting from these models, i.e. the factor by which the total counts at a station typically exceed the counts of tracked trips at this station. For half of the stations, this multiplication factor amounts to about 150, i.e. one out of 150 counts at a station corresponds to a tracked trip. However, there are also a few outliers, like the station *Donaukanal*. In a further step, we thus select those stations that suit best for estimating total daily bike trips. That is, outliers are excluded from the final estimation procedure.

As mentioned above, Eq. 7 also assumes a linear relationship between total daily tracked trips ($T_{tracked}$) and daily counts of tracked trips at stations ($CS_{tracked}$). Figure 29.a gives a visual illustration of the empirical relationship, which turns out to be nicely linear.

PUCS has received funding from the European Union's Horizon 2020 Research and Innovation Programme under Grant Agreement No. 730004

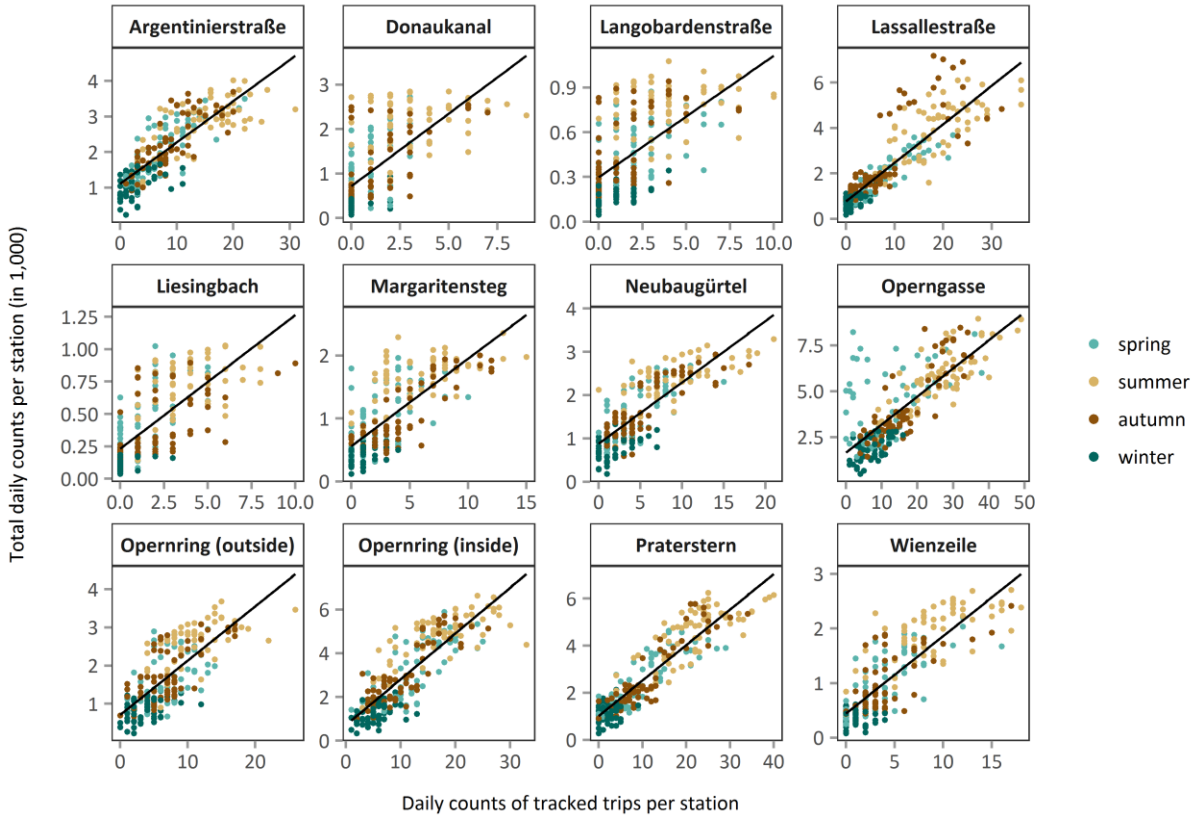

Figure 30: Relation between total daily counts per measurement station and daily counts of tracked trips per measurement station (i.e. tracks passing the respective station within 10 m distance) on workdays.

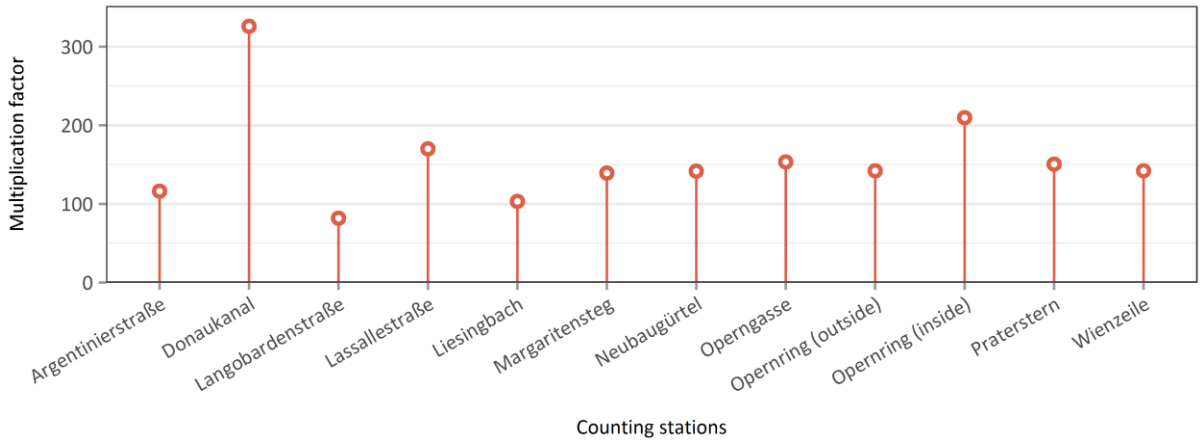

Figure 31: Factor by which total counts at a station exceed the counts of tracked trips at this station. The analysis only considers workdays.

To sum up, our pre-analyses suggest that the data sufficiently qualifies for the chosen method to provide meaningful results. Applying the described method, average daily bicycle trips on workdays in 2016 are estimated at 108,000. In addition to the annual average, Figure 29.b also shows the monthly averages of the estimated daily bicycle trips for the year 2016. For the most popular cycling month June average daily

PUCS has received funding from the European Union's Horizon 2020 Research and Innovation Programme under Grant Agreement No. 730004

trips are estimated at 149,000 in 2016, compared to 69,000 trips in the least popular cycling month January. According to the method applied, the maximum number of bicycle trips on a workday in 2016 amounted to 182,500 (07/06/2016).

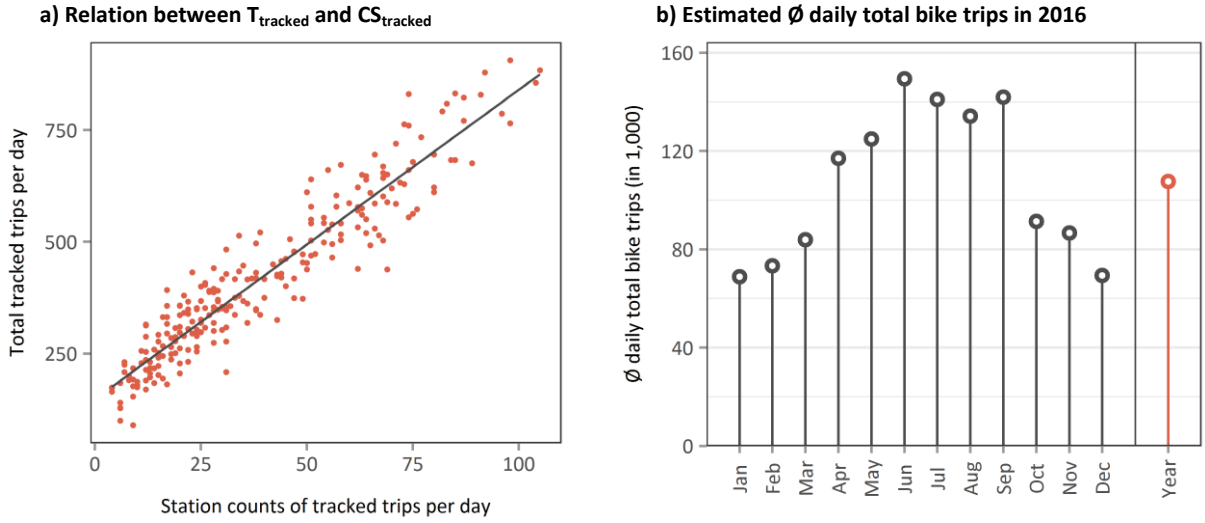

Figure 32: a) Relation between the total number of tracked trips per day ($T_{tracked}$) and the number of tracked station counts per day ($CS_{tracked}$), considering only workdays. b) Estimated average daily total bike trips on workdays in 2016.

For reasons of comparison, we also derived an estimate of the number of average bicycle trips per workday in Vienna using data from the study *Austria on the road 2013/14* (Tomschy et al. 2016). Note, however, that the study design did not aim at estimating total bike trips. According to *Austria on the road 2013/14*, each Viennese inhabitant older than 6 years has on average 2.9 trips per workday. 4 % of trips are covered by bicycle. When multiplied by the Viennese population older than 6 years, this results in an estimate of about 200,000 bicycle trips per workday.

PUCS has received funding from the European Union's Horizon 2020 Research and Innovation Programme under Grant Agreement No. 730004

8 Bibliography

Ahmed, F., G. Rose, and C. Jacob, 2010: Impact of weather on commuter cyclist behaviour and implications for climate change adaptation. Vol. 33 of, Australasian Transport Research Forum (ATRF), 33rd, 2010, Canberra, ACT, Australia https://trid.trb.org/view/1097035 (Accessed November 27, 2018).

Böcker, L., and S. Thorsson, 2014: Integrated Weather Effects on Cycling Shares, Frequencies, and Durations in Rotterdam, the Netherlands. *Weather Clim. Soc.*, **6**, 468–481, doi:10.1175/WCAS-D-13-00066.1. https://journals.ametsoc.org/doi/abs/10.1175/WCAS-D-13-00066.1.

Brandenburg, C., A. Matzarakis, and A. Arnberger, 2007: Weather and cycling—a first approach to the effects of weather conditions on cycling. *Meteorol. Appl.*, **14**, 61–67, doi:10.1002/met.6. http://onlinelibrary.wiley.com/doi/10.1002/met.6/abstract (Accessed June 15, 2016).

Brower, M. C., M. C. Barton, L. Lledó, and J. Dubois, 2013: A study of wind speed variability using global reanalysis data. https://aws-dewi.ul.com/assets/A-Study-of-Wind-Speed-Variability-Using-Global-Reanalysis-Data2.pdf (Accessed November 19, 2018).

De Ridder, K., D. Lauwaet, and B. Maiheu, 2015: UrbClim – A fast urban boundary layer climate model. *Urban Clim.*, **12**, 21–48, doi:10.1016/j.uclim.2015.01.001. http://www.sciencedirect.com/science/article/pii/S2212095515000024.

El-Assi, W., M. S. Mahmoud, and K. N. Habib, 2015: Effects of built environment and weather on bike sharing demand: a station level analysis of commercial bike sharing in Toronto. *Transportation*, 1–25, doi:10.1007/s11116-015-9669-z. http://link.springer.com/article/10.1007/s11116-015-9669-z (Accessed June 15, 2016).

European Centre For Medium-Range Weather Forecasts, 2017: ERA5 Reanalysis. doi:10.5065/D6X34W69. https://rda.ucar.edu/datasets/ds630.0/ (Accessed November 29, 2018).

Flynn, B. S., G. S. Dana, J. Sears, and L. Aultman-Hall, 2012: Weather factor impacts on commuting to work by bicycle. *Prev. Med.*, **54**, 122–124, doi:10.1016/j.ypmed.2011.11.002. http://www.sciencedirect.com/science/article/pii/S0091743511004610 (Accessed June 15, 2016).

Friedl, M. A., D. Sulla-Menashe, B. Tan, A. Schneider, N. Ramankutty, A. Sibley, and X. Huang, 2010: MODIS Collection 5 global land cover: Algorithm refinements and characterization of new datasets. *Remote Sens. Environ.*, **114**, 168–182, doi:10.1016/j.rse.2009.08.016. http://linkinghub.elsevier.com/retrieve/pii/S0034425709002673 (Accessed November 29, 2018).

Helbich, M., L. Böcker, and M. Dijst, 2014: Geographic heterogeneity in cycling under various weather conditions: evidence from Greater Rotterdam. *J. Transp. Geogr.*, **38**, 38–47, doi:10.1016/j.jtrangeo.2014.05.009. http://www.sciencedirect.com/science/article/pii/S0966692314000957 (Accessed June 15, 2016).

Lauweat, D., H. Hooyberghs, F. Lefebre, K. De Ridder, N. Veldeman, and P. Willems, 2018: Urban climate data for demonstration cases. Deliverable 5.2 of the Climate-fit.city project.

PUCS has received funding from the European Union's Horizon 2020 Research and Innovation Programme under Grant Agreement No. 730004

Marí-Dell'Olmo, M., A. Tobías, A. Gómez-Gutiérrez, M. Rodríguez-Sanz, P. García de Olalla, E. Camprubí, A. Gasparrini, and C. Borrell, 2018: Social inequalities in the association between temperature and mortality in a South European context. *Int. J. Public Health*, doi:10.1007/s00038-018-1094-6.

Phung, J., and G. Rose, 2007: Temporal variations in usage of Melbourne's bike paths. *Australas. Transp. Res. FORUM ATRF 30TH 2007 Melb. Vic. Aust. VOL 30*,. https://trid.trb.org/view/855222 (Accessed November 27, 2018).

Thomas, T., R. Jaarsma, and B. Tutert, 2013: Exploring temporal fluctuations of daily cycling demand on Dutch cycle paths: the influence of weather on cycling. *Transportation*, **40**, 1–22, doi:10.1007/s11116-012-9398-5. http://doc.utwente.nl/85633/ (Accessed July 3, 2014).

Tomschy, R., and Coauthors, 2016: Österreich unterwegs 2013/2014. Ergebnisbericht zur österreichweiten Mobilitätserhebung "Österreich unterwegs 2013/2014". [Austria on the road 2013/2014. Result report of the mobility survey "Austria on the road 2013/2014"]. https://www.bmvit.gv.at/verkehr/gesamtverkehr/statistik/oesterreich_unterwegs/downloads/oeu_2013-2014_Ergebnisbericht.pdf (Accessed June 5, 2018).

Wayne, G., 2013: The Beginner's Guide to Representative Concentration Pathways. https://skepticalscience.com/docs/RCP_Guide.pdf (Accessed November 20, 2018).

PUCS has received funding from the European Union's Horizon 2020 Research and Innovation Programme under Grant Agreement No. 730004

9 Abbreviations

BTV	Bicycle traffic volume
CE	Calendric effect
CMIP	Coupled Model Intercomparison Project
CORDEX	Coordinated Regional Climate Downscaling Experiment
ECMWF	European Centre for Medium-Range Weather Forecasts
EEA	European Environmental Agency
ERA5	ECMWF ReAnalysis 5
ME	Meteorological effect
MET	Meteorological
PRH	Hours with precipitation (precipitation hours)
RCP	Representative Concentration Pathway
SD	Snow depth
WBGT	Wet-bulb globe temperature
WS	Wind speed

PUCS has received funding from the European Union's Horizon 2020 Research and Innovation Programme under Grant Agreement No. 730004

PUCS has received funding
from the European Union's Horizon 2020
Research and Innovation Programme
under Grant Agreement No. 730004